UNIVERSITAT DE BARCELONA

Final Degree Project

Biomedical Engineering Degree

New Nickel-Titanium alloys for biomedical applications

Barcelona, 14th June 2021

Author: Carles Garí Crespí

Director/s: Dr. Javier Fernández González

Tutor: Dr. Javier Fernández González

ABSTRACT

Nitinol is a shape memory alloy with unique shape memory characteristics and superelasticity.

The understanding of these properties as well as its main applications in the biomedical field are the central object of study of this final degree project. Special emphasis is placed on cardiac devices composed of this alloy such as heart valves and coronary stents. Due to its distinctive properties, the use of these nitinol-based devices has allowed to successfully treat certain cardiovascular pathologies, such as interventricular communication and peripheral vascular diseases.

However, surface roughness of nitinol stents represents an important factor to consider since it considerably affects its biocompatibility. The friction of the implant in contact with the vascular tissue can cause the adhesion of proteins and therefore, lead to thrombus formation.

With the aim of improving its biocompatibility, effective surface treatments in reducing surface roughness of nitinol stents are explored. Among many alternatives, the electrochemical procedure known as electropolishing is analysed in detail in this project.

To test the effectiveness of this surface treatment, an experimental procedure based on the electropolishing of nitinol stents under different conditions is performed. A meticulous characterization process of the surface of the samples is then carried out. The optimal polishing conditions are determined, thus achieving a considerable reduction in the surface roughness of nitinol stents.

TABLE OF CONTENTS

LIST OF FIGURES

LIST OF TABLES

GLOSSARY

SMA: Shape memory alloy

Ra: Average roughness

VSD: Ventricular septal defect

LV: Left Ventricular

PAH: Pulmonary arterial hypertension

CHF: Congestive heart failure

Ms: Martensite Start

Mf: Martensite finish

As: Austenite Start

Af: Austenite finish

MIT: Tension-induced martensite

Md: MIT's maximum training temperature

SE: Self-expanding (SE)

PVD: Physical vapor deposition

EP: Electropolishing

H_3PO_4: Phosphoric acid

H_2S0_4: Sulfuric acid

IEG: Interelectrode gap

TiO_2: Titanium oxide

SEM: Scanning electron microscopy

OM: Optical microscopy

AFM: Atomic force microscopy

NaCl: Sodium chloride

SMST: Shape Memory and Super elastic Technologies Society

HNO_3: Nitric acid

SPM: Scanning probe microscopy

WBS: Work breakdown structure

SWOT: Strengths, Weaknesses, Opportunities and Threats analysis

FDA: Food and Drug Administration

PMA: Premarket approval

AEMPS: Spanish Agency for Medicines and Medical Devices

1. INTRODUCTION

1.1. INTRODUCTION

There are a wide variety of malformations and structural alterations of the heart and cardiovascular system that give rise to dysfunctions of the circulatory system. In many cases, especially in the most severe ones, interventions need to be carried out using different types of implants, whether biological or synthetic. That is why, today, there is a wide variety of biomaterials to treat cardiovascular diseases that offer a wide range of possibilities because of the properties they present. Elements used as implants for the cardiovascular system include biological processed materials, plastics, ceramics and different metals and alloys. Because they are subjected to loads either by static or repetitive, they require an excel combination of strength and ductility [1]. Among different biomaterials , metals are considered more advantageous in cardiovascular applications due to their remarkable properties including high impact strength, high ductility, and high strain energy [1].

Metals such as stainless steel or titanium have been used in various types of cardiac implants [2]. However, it is vitally important to mention shape memory alloys (SMA), because of the unique thermomechanical properties they present. This collection of metal compounds are able to experience large deformation and recover its original shape when exposed to a specific external stimulus [3]. Consequently, implantable cardiac devices such as stents or heart valves can be deformed into relatively small size before they are implanted into the human body during minimally invasive surgery (MIS)[4]. Once they are exposed to body temperature, these metallic devices expand and recover to a larger shape.

In addition to their thermomechanical behaviour, SMA have high biocompatibility, so they are an excellent option for cardiovascular applications. SMA generally used are copper-based, iron-based and nickel-based [3]. However, the binary equiatomic nickel titanium alloy (nitinol) is the preferred material since it has higher thermal cycle properties and yield stress [5].

For this reason, nitinol is, among all SMA, the one which has received more development effort. Nowadays, nitinol is used in various cardiovascular procedures, including transcatheter valve replacement, as coronary self-expandable stents, or as closure devices in several cardiac pathologies, such as ventricular or atrial septal defects. Nevertheless, the most obvious and widely used application of nitinol has been in the design of stents for stenotic or blocked blood vessels [6].

However, the long-term implantation of metallic stents is associated with restenosis and thrombosis. The thrombogenic potential of nitinol itself has been a long controversy in the science community [5]. The cause of this controversy however, was concluded to be caused by the variations in surface preparation and topography during manufacturing and sterilization procedures of nitinol stents [7].

The production and manufacture of nitinol stents requires high precision since its surface quality has a significant influence on biocompatibility. If the surface of the cardiac device has a poor surface quality, there is a risk that the introduced material will cause damage in patients as thrombi, among other complications.

That is why, to improve the biocompatibility of nitinol stents, surface treatments must be carried out, thus eliminating any type of impurity that exists on the surface itself. Therefore, a higher quality and more polished surface is achieved, creating also a non-reactive layer, usually of oxide, protecting the material from damage caused by the environment.

Electropolishing is an electrochemical process that is presented as an alternative of special interest for the improvement of the metallic implant surface. This procedure decreases roughness, achieving a smoother and polished surface. While less precise methods of finishing, like tumbling, vibro-finishing, or hand deburring, may be effective in some cases, none can match electropolishing for its ability to achieve the highest-quality surface finish with microscopically precise results [8].

In this project, a detailed literature review about the biomedical applications of the SMA nitinol has been carried out. Specifically, special emphasis has been placed on cardiac devices such as coronary stents, heart valves and other devices composed of nitinol. In addition, severe cardiovascular pathologies which can be treated by using this specific kind of devices have been studied in detail.

To carry out this bibliographic review, a wide variety of scientific articles collected in different databases have been consulted, among which are ScienceDirect, Elsevier, PubMed and so on. In addition, those articles with a publication date of not less than 15 years have been selected, but also some exceptional cases of some articles with more antiquity are included, since they have been considered as of vital importance for the development of this work.

Once it has been analysed in detail the use of devices manufactured with this alloy and the advantages and disadvantages they present in the biomedical environment, an experimental procedure has been carried out in the laboratory. The experimental procedure performed is an electropolishing of Nitinol coronary stents to decrease the surface roughness of the samples. The objective is to achieve a polished surface to improve the biocompatibility of the sample by reducing the friction of the implant in contact with the vascular tissue and the adhesion of proteins that may induce thrombi.

The most decisive parameter and which this work is focused on is the Average Roughness (Ra) of the samples, which measures the overall height of the surface texture. This parameter is defined as the average value of the height of the surface profile above and below a centreline throughout a prescribed sampling length [9].

Once the electropolishing process is finished, quality images of the processed samples will be obtained. In addition, by using a specific software, roughness parameters will be extracted to determine the most optimum electropolishing conditions with which the lowest Ra value is obtained.

.

1.2. PROJECT OBJETIVES

This final degree project is a bibliographic project improved with the addition of a selected experiments to study the industrial feasibility of the concepts described. The objectives of this project are:

- To make an **extensive bibliographic documentation** on the properties and use of the SMA nitinol and its main applications in the biomedical field.
    - Placing special emphasis on cardiovascular devices composed of this alloy such as vascular stents or heart valves and their biocompatibility problems associated.
    - To understand cardiovascular pathologies as interventricular communication or peripheral vascular diseases and their treatment using nitinol-based implants.
- **To create an experimental procedure** to reduce the average roughness (Ra) of commercial coronary stents.
    - Characterize the surfaces obtained.
    - Select the optimum conditions on electropolishing process.

1.3. SCOPE AND SCAN

This project has been performed over a period of approximately 7 to 8 months, between November 2020 and June 2021. During the first 3-4 months the documentation and bibliography tasks were carried out while the last months were dedicated to the implementation of all the knowledge learned, performing the experimental part in the laboratory. Although time to develop the project was limited, significant results have been achieved in terms of reducing the average roughness (Ra) of the treated samples.

It should also be noted that structuring this work as a true engineering project has allowed to understand and go into detail in other relevant aspects within the development of a project. This is case of the market analysis, technical feasibility, the chronogram prevision and so on. These sections also have a significant importance in the development of a project, and therefore special attention should be paid to them, in addition to the experimental procedure and the bibliographic documentation carried out.

2. BACKGROUND

2.1. CARDIOVASCULAR PATHOLOGIES

This section presents two specific cardiovascular pathologies which can be treated by using two different cardiovascular nitinol-based devices.

- On one hand, **interventricular communication** is a common cardiovascular pathology which can be treated by using **nitinol closure devices.**
- On the other hand, **peripheral vascular disease** is a pathology that can be treated successfully by using **self-expandable nitinol stents.**

2.1.1 INTERVENTRICULAR COMMUNICATION

2.1.1.1 GENERAL CONTEXT

Interventricular communication consists of the most common congenital heart disease and can be detected during the prenatal, postnatal, during childhood or during the adult stage. It is estimated to be responsible for 30% of congenital heart disease in the child population and appears in 1-5% of live births [10].

This pathology occurs when there is an abnormal development or an interruption of the interventricular septum formation during the embryogenic heart morphogenesis. During the pregnancy, the left and right ventricles of the fetus heart are not separated. As the fetus grows, an interventricular septum is formed to separate both the right and the left ventricles. The ventricular septum consists of a curved structure divided into 2 morphological components, the membranous septum and the muscular septum [11] .

The membranous septum is a small structure located at the base of the heart between the inlet and outlet components of the muscular septum. The muscular septum is a non-planar structure composed of 3 different parts: the infundibular, atrioventricular and the inlet components. If the ventricular septum does not fully form, there is a hole left known as **Ventricular Septal Defect (VSD).** Different views of VSDs seen from the right and left ventricular aspects can be appreciated *(see Fig 1.).*

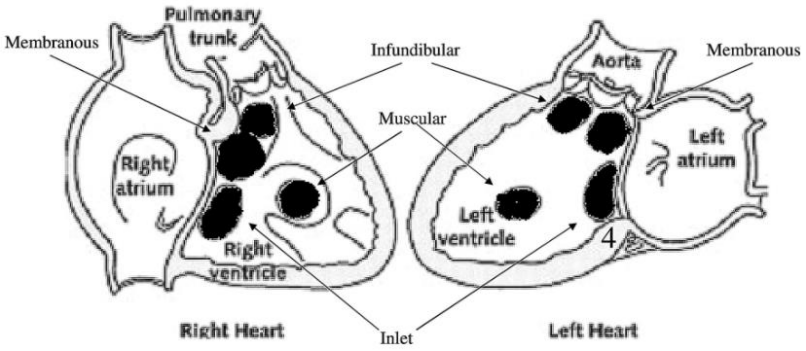

Fig 1. *Locations of VSDs seen from the right and left ventricular aspects [10].*

Most VSDs are restrictive (<5 mm) and undergo spontaneous closure during the first year of life [12]. It is common that the new-born has no symptoms, and the hole can be closed over time to as the interventricular septum continues to grow after birth.

The incidence of spontaneous ventricular septal defect (VSD) closure varies greatly, depending on the age and gender of subjects at spontaneous closure, the size and site of the defect, the types of defect, as well as the population studied, methods employed, and length of follow-up period [13]. Small defects may not have hemodynamic consequences, but the presence of a significant left-to-right shunt can cause left ventricular (LV) overload, pulmonary arterial hypertension (PAH), ventricular dysfunction, arrhythmias, and aortic regurgitation [14].

2.1.1.2 REPAIR SURGERIES

Approximately 85% to 90% of small isolated VSDs close spontaneously during the first year of life. Patients with small, asymptomatic VSDs with the absence of PAH have an excellent prognosis without any intervention.

However, cases in which children have larger VSD, surgical repair procedures are recommended even though they still have no symptoms. These procedures are vitally important as they can prevent future complications such as heart failures, due to the increase workload of the heart, or arrythmias, in which the heart's normal electrical activity is affected.

Treatment of VSDs has improved dramatically over the last 50 years. Patch closure of a ventricular septal defect through sternotomy, with cardiopulmonary bypass, has been done for more than 50 years. However, although open-heart surgery is considered a standard treatment for VSDs, catheter-based intervention is a promising alternative [15].

A study performed by Yang et al [15] compared the safety and efficacy of the 2 intervention methods for VSDs in children. In this study, it was concluded that surgical repair and transcatheter device closure were effective treatments, with excellent midterm outcomes. However, transcatheter device closure was selected as the treatment of choice, as it presented fewer myocardial injuries and transfusions, shorter hospital stays, reduced medical costs, and faster recovery times.

2.1.1.3 IMPLANTS USED

As it was proved, transcatheter device closure is a better method of intervention than the traditional surgical repair, with super fewer complications in patients.

There are a wide variety of transcatheter closure devices that can be used for this specific type of surgery. Among all the different alternatives, it is important to highlight closure devices made with nitinol, the metal alloy composed of Nickel (Ni) and Titanium (Ti).

Closure devices, as well as other cardiac devices composed of this characteristic material, stand out for their high biocompatibility, high resistance to fatigue, resistance to corrosion and so on.

Nitinol VSD closure devices have allowed over 50,000 patients with congenital heart disease to undergo nonsurgical closure of these significant congenital heart defects [15]. *Fig 2.* shows the Shanghai pmVSD-O, which consists of a symmetrical double-disk device made of 0.005 in. nitinol wire mesh and fabric inside.

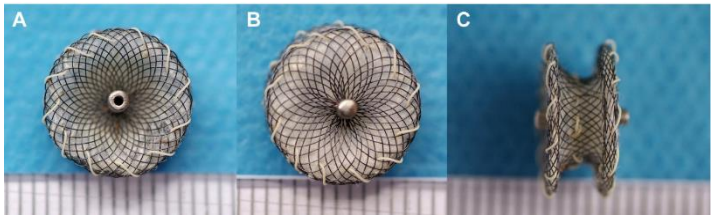

***Fig 2**. Front view (A) back view (B) and lateral view (C) of peri membranous ventricular septal defect occluder made of 0.005 in. nitinol wire mesh* [15]

2.1.2 PERIPHERAL VASCULAR DISEASE (PAD)

2.1.2.1 GENERAL CONTEXT

Peripheral vascular disease (PAD) is one of the most prevalent cardiovascular conditions worldwide. It affects nearly 200 million people around the world with increasing global importance due to longer life expectancy and prolonged risk factor exposure [16].

PAD consists of a chronic and progressive atherosclerotic disease which leads to a partial or total peripheral vascular occlusion. PAD affects blood vessels in areas external to the heart. Therefore, the organs which receive the blood supply through these vessels, such as the brain, heart, and legs, may not receive adequate blood flow for their normal functioning. This disease is associated to high risk fatal and non-fatal cardiovascular events frequently occurring, such as myocardial infarction and stroke [17].

The most common cause of this disease is atherosclerosis (plaque build-up inside the walls of the arteries), as it reduces the amount of blood flowing to the extremities as well as the oxygen and nutrients to tissues. Atherosclerosis plaque is made up of deposits of fatty substances, cholesterol,

and waste products from cells. The build-up of this plaque is a gradual process, so, over time, vessels become narrowed, blocked, or weakened.

Risk factors associated to PAD may be divided into reversible and irreversible categories [16]. However, the main risk factors associated are diabetes, hypertension , smoking and hyperlipidaemia, as they are also involved in 80-90 % of the cardiovascular diseases [18].

2.1.2.2 TREATMENT USING CORONARY STENTS

The treatment to be used depends on the severity of the blockage or narrowing of the affected arteries. If the degree of obstruction is not severe, the recommended treatment is to adopt changes to achieve a healthy lifestyle. However, when obstruction becomes severe, treatment may be based on medication or on a surgical procedure.

Due to this project is mainly focus on cardiac devices including coronary stents, the treatments that require this type of interventions are studied.

Angioplasty is a non-surgical intervention which can be used for treating occluded or narrowed blood vessels, restoring the correct blood flow. To carry out this procedure, a catheter (thin flexible guidewire) is introduced normally through the femoral artery until it reaches the corresponding blockage. During this process, guiding is performed using X-ray imaging. Moreover, a balloon tipped catheter is then passed over the guidewire and pushed along it until the balloon reaches the occlusion or stenosis [19]. Finally, the balloon is inflated so the blocked vessel opens and widens.

To prevent the vessel from closing again, a **stent**, a small mesh tube, is placed.

Stents are vascular prostheses used to facilitate circulation in narrowed or clogged blood vessels and thus facilitate the passage of blood through them. Nowadays, different types of stents can be found, depending on the materials used for its manufacture or according to its implementation.

The two main types of stents are:

- **Balloon-expandable:** The angioplasty balloon is employed to both open the blocked vessel and expand the stent [19].

- **Self-expanding:** The stent is pushed out of the catheter exerting its self-expanding force. Then, opens out immediately to support the already dilated lumen. This type of stents have proven to reduce the extent of arterial recoil and restenosis as compared to balloon angioplasty procedures and provide a less invasive alternative in the treatment of endovascular disease [20].

Flexibility is the most important characteristic of vascular stents, However, there are other additional requirements that must also be met: high radial strength, low elastic deformation, small diameter, and the possibility of monitoring through the bloodstream, among others [21].

Materials with super-elastic and shape-memory properties, such as nitinol, meet these requirements and are ideal materials for the manufacturing of stents.

Nitinol is an attractive material which facilitates the positioning of stents for a precise implantation. Moreover, the narrow temperature range within which nitinol's super-elasticity is exhibited includes body temperature. Thus, nitinol has become the material of choice for the design of self-expanding (SE) stents [22].

As explained previously, SE stents are compressed at the moment of being inserted into the body and once they are positioned correctly, they are self-expanded to the original position.

Specifically, mechanical deformation of the original piece is performed (as initially it does not fit inside the vessel). Once inside the vessel, the body itself heats the alloy and widens again. *Fig 3.* and *Fig 4.* show the design and deployment system of a nitinol stent. Moreover, in *Fig 5., the* crimped and expanded configuration of a nitinol stent inside a vessel is displayed.

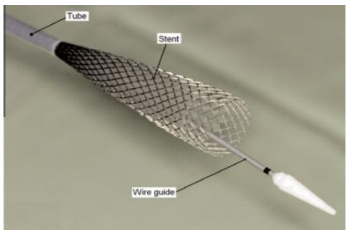

Fig 3. *Manufactured nitinol stent [20].*

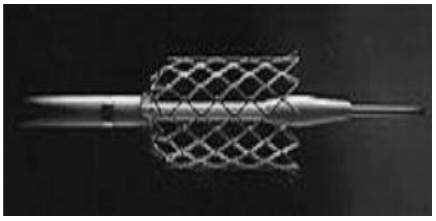

Fig 4. *Deployment system of a nitinol stent* [23].

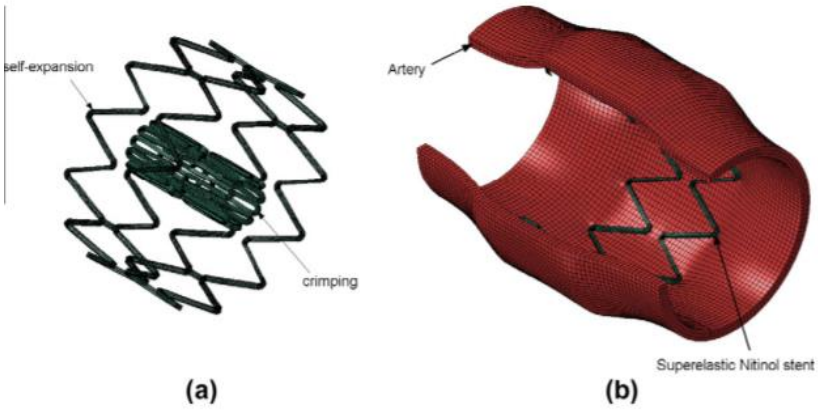

Fig 5*. (a) Crimped and expanded configuration of the nitinol stent (b) Expansion of the artery after superelastic nitinol stent deployment [20]*

2.2 THE SHAPE MEMORY ALLOYS

This section describes the shape memory alloys as well as the basic principles of their most distinctive properties: the shape memory effect and super elasticity.

2.2.1 SMA: GENERAL ASPECTS

A shape-memory alloy (SMA) is an alloy that remembers its original, cold-forged shape by returning to that pre-deformed shape when heated [24]. As its name suggests, and unlike traditional metals, these group of alloys are able to return to their original form (shape or size) when subjected to a memorisation process between two transformation phases, which is temperature or magnetic field dependent [25].This statement means that these materials can be plastically deformed at some relatively low temperature, and upon exposure to some higher temperature will return to their shape prior to the deformation [26].

The two unique properties these alloys have are the shape memory behaviour and the super-elasticity. **Shape memory behaviour** means that the original shape can be recovered after deformation by heating the alloy. On the other hand, **super-elasticity property** enables that any apparent plastic deformation can be returned to the original shape by releasing the load.

These materials can have a **one-way shape memory** if they exhibit this behaviour only upon heating, or, a **two-way shape memory**, if they are also able to change their shape upon recooling [26]. There are a variety of alloys which have been developed over the years and exhibit the shape memory behaviour *(see Table. 1.)* but only those that can recover substantial amounts of strain are of commercial interest [26].

Alloy	Composition	Transformation-temperature range °C	Transformation-temperature range °F	Transformation hysteresis Δ°C	Transformation hysteresis Δ°F
Ag-Cd	44/49 at.% Cd	−190 to −50	−310 to −60	≈15	≈25
Au-Cd	46.5/50 at.% Cd	30 to 100	85 to 212	≈15	≈25
Cu-Al-Ni	14/14.5 wt% Al 3/4.5 wt% Ni	−140 to 100	−220 to 212	≈35	≈65
Cu-Sn	≈15 at.% Sn	−120 to 30	−185 to 85		
Cu-Zn	38.5/41.5 wt% Zn	−180 to −10	−290 to 15	≈10	≈20
Cu-Zn-X (X = Si, Sn, Al)	a few wt% of X	−180 to 200	−290 to 390	≈10	≈20
In-Ti	18/23 at.% Ti	60 to 100	140 to 212	≈4	≈7
Ni-Al	36/38 at.% Al	−180 to 100	−290 to 212	≈10	≈20
Ni-Ti	49/51 at.% Ni	−50 to 110	−60 to 230	≈30	≈55
Fe-Pt	≈25 at.% Pt	≈−130	≈−200	≈4	≈7
Mn-Cu	5/35 at.% Cu	−250 to 180	−420 to 355	≈25	≈45
Fe-Mn-Si	32 wt% Mn, 6 wt% Si	−200 to 150	−330 to 300	≈100	≈180

Source: Ref 5

Table. 1. *Different metal alloys with shape memory effect* [26].

The three main types of SMAs are the copper-zinc-aluminum-nickel, copper-aluminum-nickel, and nickel-titanium (nitinol) alloys, but SMAs can also be created by alloying zinc, copper, gold, and iron [24].

2.2.2 HISTORY OF SHAPE MEMORY ALLOYS

As for history, it should be noted that materials with shape memory began to be known in 1932 by Chang and Read [26], who observed reversibility of the transformation in AuCd by metallographic observations and resistivity changes. In subsequent years, further observations of these unusual properties occurred in 1938 on a Copper and Zinc (Cu-Zn) alloy and in 1951 in a bent bar of AuCd.

However, it was not until much later, that serious advances occurred and the discovery of these properties in equiatomic nickel-titanium took place [26].

More precisely, it was in 1958 that the SMA nitinol had its origins, when William Buehler, a supervisor at the Naval Ordnance Laboratory (NOL) had to select from a set of metal alloys for the tip cones of submarine missiles. Nitinol was finally chosen, as it exhibited considerably more impact resistance and ductility than the other eleven alloys [27]. The alloy was named Nitinol, combining Nickel (**N**i) and Titanium (**T**i) as its constituent elements, in addition to Nol, which refers to the **N**aval **O**rdnance **L**aboratory, where it was discovered.

However, it is important to note that, one of the most important properties of the SMA, the shape memory behaviour, was not discovered until later. When, in 1961, during a laboratory management meeting, long thin strips of Nitinol were prepared. Consequently, the trips were bended longitudinally, and in order to demonstrate material's unique fatigue-resistant properties, the samples were compressed and stretched continuously without breaking. The discovery of the shape memory behaviour happened, when suddenly, one of the compressed samples was heated using a pipe lighter, and consequently, the nitinol strip stretched out longitudinally thus resulting in the discovery of this vitally important property [27].

Later, a series of experiments were performed, which confirmed that the SMA properties in hot and cold form were different, and due to this change in temperature, a structural transformation of its atoms was produced.

2.2.3 SMA PROPERTIES

2.2.3.1 SHAPE-MEMORY EFFECT

Alloys with shape memory and super elasticity are associated with a phase transformation in solid state, the **thermoelastic martensitic transformation**. In this type of alloys, the term austenite, or Beta phase, is used for the stable phase at high temperatures, which has a high crystallographic symmetry, while the term martensite is used for the stable phase at low temperatures. Martensite is also characterised by having a low crystallographic symmetry.

The crystalline structure of the two phases of the SMA depending on the temperature can be appreciated in *Fig 1.* [28].The austenitic crystalline structure is a cubic structure centred on the body, while the martensitic has a more complex rhomboid structure.

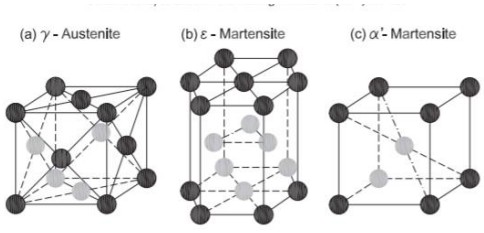

***Fig 6**. Crystalline structure of the two phases of alloy* [28].

Ms and **Mf** (Martensite Start and Martensite finish) can be defined as those start and end temperatures of the martensitic transformation, as well as **As** and **Af** (Austenite Start and Austenite finish) are the start and end temperatures of the austenitic transformation.

With temperatures below Ms, the martensitic phase begins to be more stable than the austenitic phase, so between Ms and Mf there is a coexistence of the two phases. Once temperature is below Mf, the material presents only martensitic phase.

The difference between transition temperatures during heating and cooling is called **hysteresis**. It is defined as the difference between the temperatures at which the material has transformed into 50% of austenite during heating and 50% of martensite during cooling. Playing with these start and end temperatures of the martensitic and austenitic phases, if a material is deformed below Mf, it will be able to return to its initial form by heating above Af. This process described can be appreciated in *Fig 2.* , in which the hysteresis with shape memory transformation temperatures are displayed [29].

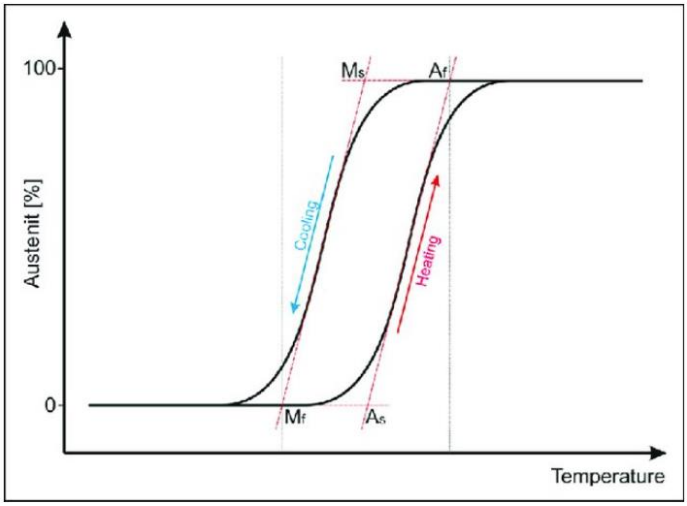

***Fig 7**. Hysteresis with shape memory transformation temperatures* [29].

Thermoelastic martensitic transformation is a solid-state transformation without diffusion. This means that atoms are redistributed together to form a more stable crystalline network. The transformation of austenite into martensite occurs in two stages. In the first stage, the crystallographic structure is moved by shear movements as it can be seen in *Fig 8.* [30].

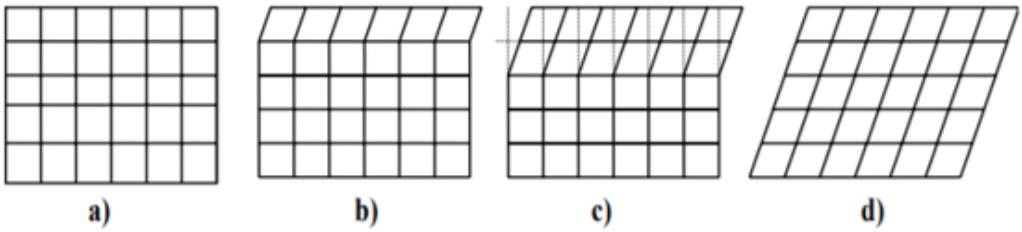

***Fig 8**. First stage of the martensitic transformation, shearing process. Progression from the austenitic structure to a completely martensitic structure* [30].

In this situation the austenite must self-accommodate to minimize energy in its new state. For this self-reduction to be reversible, it must be given by means of a twinning mechanism *(see Fig 9.).*

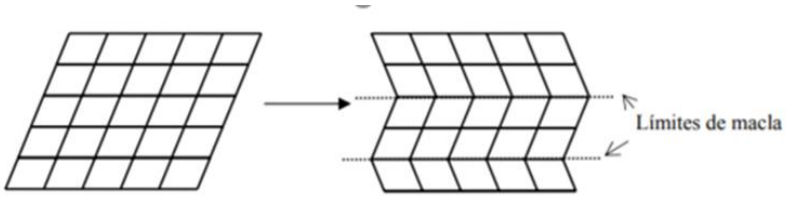

***Fig 9**. Second stage of thermoelastic martensitic transformation, twinning process. Two variations of martensite exist* [30].

Martensite can have two shapes, twinned and detwinned. It is important to note that the generated martensite plates can appear with 24 different orientations being a phase of low crystallographic symmetry, while the austenitic phase, being a phase of high crystallographic symmetry, has only one way to orient itself. So, the transformation sequence, seen from a macroscopic point of view, *(see Fig 10.),* would follow the following order:

1- Element in austenitic phase being above Af.

2- When cooling below Mf the material retains its original shape in the martensitic phase because the generated martensite plates have 24 orientations to accommodate, and no material shape change is needed.

3- Being at a temperature below Mf, the material can be deformed by having a structure where the plastic deformation happens by a movement of the martensite plates, not by the dislocations of the material.

4- When heating up to a temperature above Af, an austenitic structure is achieved, recovering the original shape of the material since, as the austenitic phase has a high crystallographic symmetry (and only one way back instead of the 24 one way), the only way the material must have an austenitic structure is to get the atoms back to their initial position [30].

Fig 10. shows the one-way effect nitinol transformation with temperature [31].

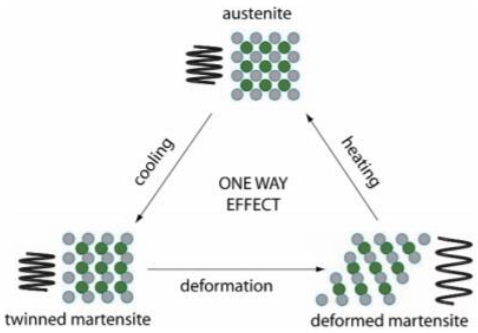

***Fig 10.** One-way effect nitinol transformation with temperature* [31].

2.2.3.2 SMA SUPERELASTICITY

Martensitic transformation cannot occur only by a change in the temperature of the material but can also occur when applying a tension to the material.

When applying a load, martensite can form above Ms, in this case the martensite that forms is called tension-induced martensite (MIT).Therefore, Md is defined, the maximum temperature above which no martensitic can occur [30].

Super elasticity occurs in the temperature range from As to Md. In this temperature range, martensite is stable when applying some tension, but becomes unstable when that same tension is no longer applied. At a temperature higher than Md, if a tension is applied to the shape memory alloy, martensite is no longer produced, but the material is plastically deformed [32].

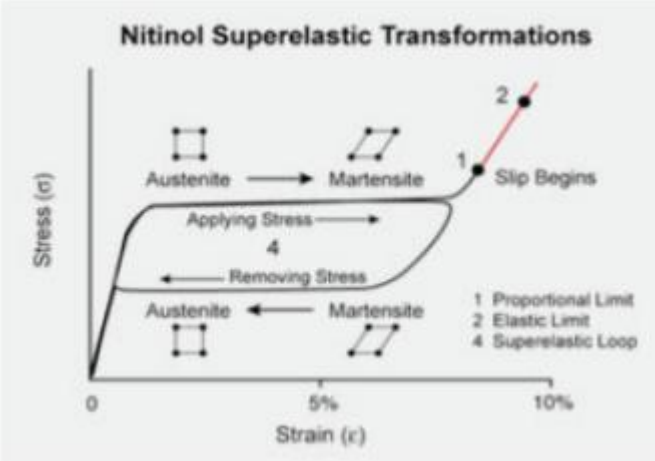

***Fig 11**. Nitinol super elastic transformations* [32].

When applying load, the material deforms elastically, the austenitic phase deforms at first, but then is observed that, without applying much tension, the material deforms a lot, this is because the austenite transforms into martensite.

When austenite is monocrystalline, martensite plates can be moved virtually along the material and elastic deformations of up to 10% can be obtained. Whereas if austenite is polycrystalline, the extent of martensite plates is limited by the presence of grain boundaries, so elastic deformation is limited to 8%.

When the stress is released, as the deformation is elastic, the martensite plate reverts to austenite and the original shape is recovered.

The following graph (*see Fig 3.*) shows in summary, the behaviour that SMA can adopt depending on the temperature [30].

- In **A** curve, the material is at a temperature above Md, in austenitic phase. Therefore, it behaves like a conventional material subjected to stress until it breaks. As for its curve, it presents a first

linear section corresponding to the elastic deformation and another section that belongs to the plastic deformation and breakage.

- **B** curve represents the shape memory effect. If the material is subjected to stress in martensite phase, a considerable deformation occurs. However, this deformation is fully recovered by subjecting the material to a heating process.

- **C** curve corresponds to the superelasticity behaviour. The material is in the austenitic phase, above Af. The horizontal section corresponds to the formation of stress-induced martensite. At the end, when applying tension, a plastic deformation region appears. If this tension is released, the material can recover its initial shape without any heating process.

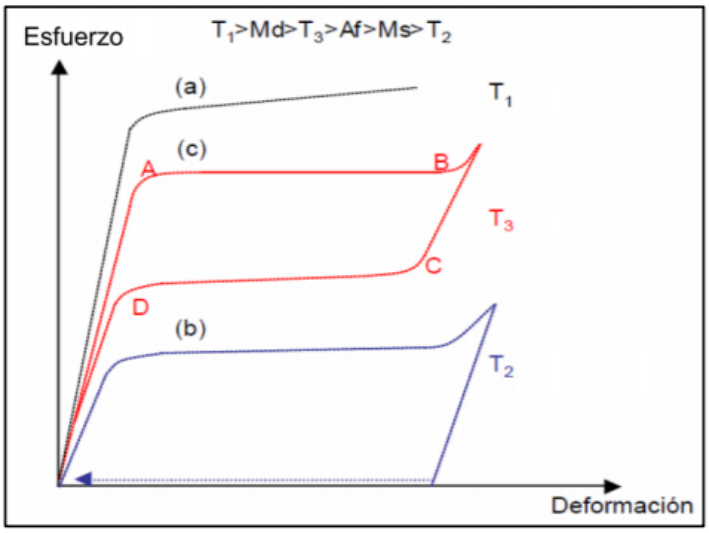

***Fig 12**. SMA behaviour depending on temperature* [30].

2.3 NITINOL ALLOY

Once the two most important properties of SMA have been explained in detail, nitinol and its distinctive properties will be studied, in addition to describing its main applications.

NiTi alloys (nitinol) consist of alloys which contain almost equal atomic amounts of Ti and Ni (49–51 mol%Ni). It is the most common material among all SMA and presents good mechanical and physical properties, as well as good corrosion and fatigue resistance. Moreover, as a SMA, it exhibits the common characteristics of these alloys, both shape memory effect and superelasticity, being able to adopt deformations of up to 8-10% [30].

It is important to mention that nitinol has greater shape memory strain (up to 8%) , tends to be much more thermally stable and has excellent corrosion resistance compared to other shape memory alloys [26].

2.3.1 MAIN NITINOL APPLICATIONS

Nitinol offers a wide variety of possibilities. Despite having many applications in industry, it is in the field of medicine in which the contribution of this material is most appreciable.

The combination of shape memory effect and superelasticity with good biocompatibility comparable (or better) to that of Ti, made Nitinol especially suitable for medical applications [33].

Depending on the role to be performed and considering the properties of the material, different biomedical devices can be designed and manufactured by controlling the processing temperatures of nitinol alloys.

-Cardiovascular applications: The shape memory effect and superelasticity are very interesting properties for the manufacturing of cardiovascular devices. In particular, the manufacture of self-expanding stents is one of the most widespread applications with most relevant commercial use. As previously explained, self-expanding coronary stents are used to treat aneurysms or diseases of arterial occlusions.

Moreover, nitinol closure devices represent another type of cardiovascular devices fabricated with this alloy. As previously explained, closure devices can be used to treat severe pathologies such as the interventricular communication or other septal defects.

-Orthopaedics applications: Another field where nitinol medical devices can be used is in orthopaedics. In particular, nitinol is used to manufacture osteosynthesis plates for internal fixation of bones, staples, intervertebral artificial joints among many others [34].

-Orthodontics applications: Moreover, super elasticity property is of great interest in the field of orthodontics with the manufacturing of corrective wires to move and reposition teeth.

In addition, thanks to recent advances and innovations in the research and development of this material, medical devices made with nitinol have experienced a great expansion in different therapeutic areas, such as the manufacture of microbombs that can replace functions of the heart or kidney [30].

2.3.2 NITINOL PROPERTIES

Nitinol presents both physical and mechanical properties which make this alloy an ideal material for all the applications described previously.

Table. 2. summarizes some of the most important physical and mechanical properties of this alloy, including its melting temperatures, resistivity, young's modulus and so on. These properties are strongly dependent on the processing history and play an important role in the design and manufacturing of several devices, including self-expanding stents [35].

Properties	Property value
Melting temperatures, °C (°F)	1300 (2370)
Density, g/cm³ (lb/in.³)	6.45 (0.233)
Resistivity, μΩ · cm	
Austenite	≈100
Martensite	≈70
Thermal conductivity, W/m · °C (Btu/ft · h · °F)	
Austenite	18 (10)
Martensite	8.5 (4.9)
Corrosion resistance	Similar to 300 series stainless steel or titanium alloys
Young's modulus, GPa (10^6 psi)	
Austenite	≈83 (≈12)
Martensite	≈28–41 (≈4–6)
Yield strength, MPa (ksi)	
Austenite	195–690 (28–100)
Martensite	70–140 (10–20)
Ultimate tensile strength, MPa (ksi)	895 (130)
Transformation temperatures, °C (°F)	−200 to 110 (−325 to 230)
Latent heat of transformation, kJ/kg · atom (cal/g · atom)	167 (40)
Shape memory strain	8.5% maximum

Table. 2*. Physical and mechanical properties of nitinol* [26].

Many materials have mechanical properties very different from those of the human body. Stainless-steel is a clear example, which has a very limited elastic deformation strain. *Fig 13.* compares the elastic strain both for nitinol and 316 stainless steel, in which the superelastic behaviour of nitinol is clearly appreciated [36].

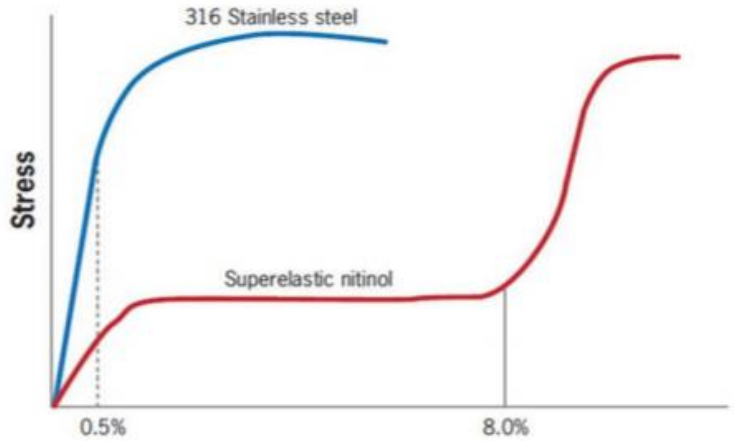

Fig 13*. Comparison between elastic strain for nitinol and 316 Stainless steel* [36].

Fig 14. displays the deformation characteristics of nitinol and living tissues. As it is appreciated, nitinol has a stress-strain curve very similar to some tissues.

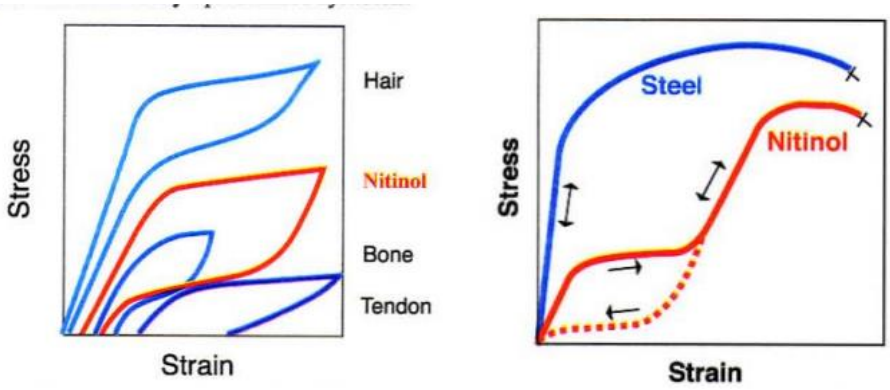

***Fig 14**. Biomechanical compatibility of nitinol: Deformation characteristics of nitinol and living tissues* [35]. ***Fig 15.** Stress-strain diagram for Nitinol and stainless steel* [30].

Moreover, *Fig 15.* shows a characteristic strain/stress curve of a nitinol alloy at body temperature. As it is displayed, nitinol shows a different behaviour compared stainless steel.

After an initial linear increase in stress with strain, large strains can be obtained with only a small further stress increase [35] .This corresponds to the loading plateau, the end of which is reached at 8% strain *(see Fig 13.)*. Unloading from the end of this point causes the stress to decrease rapidly until a lower plateau is reached (unloading plateau) [35]. Consequently, strain is recovered with a small decrease in stress.

To apply this concept in a more practical way, *Fig 16.* is presented, showing stress hysteresis property of nitinol. This graph follows the cycle of crimping a nitinol stent into a delivery system, deploying it and have it expand and interact with the vessel [35]. Now the strain (X) axis is converted into the stent diameter whereas the stress (Y) axis corresponds to the hoop force.

Point **A** corresponds to the original size of a stent, which is larger than the vessel. Stent is then crimped into the delivery system, which corresponds to point **B**. Once the stent is delivered to the target size, it expands from point **B** until it reaches point **C**.

At this point further expansion of the stent is prevented and because the stent has not recovered its original full size, it continues to exert a low outward force known as Chronic Outward Force **(COF)**, a measure of the radial force the stent projects outward in its deployed configuration [36].

The stent is able to resist any kind of external compression forces, including Radial Resistive Forces **(RRF)**, consisting of the force required to compress the stent radially.

COF and RRF determine the force balance between the stent and the wall vessel [36].

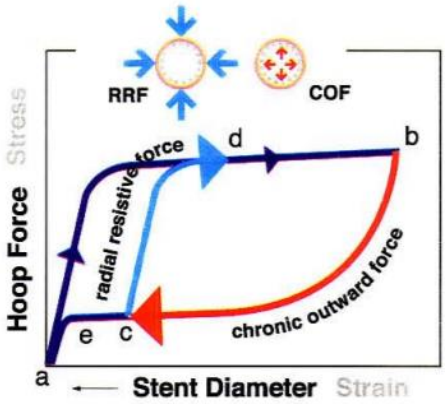

***Fig 16**. Schematic stress hysteresis demonstrated with the cycle insertion into delivery system/deployment/compression of a stent* [36].

2.3.2.1 FATIGUE RESISTANCE

Fatigue is an important factor to consider in cardiovascular applications. Fatigue tests can be performed under two different test conditions, at constant deformation and at constant stress. Nitinol presents a great resistance under large deformations, however, under constant tensions the failure occurs much earlier. For this reason, most fatigue studies plot fatigue life as a function of strain (see *Fig 17.)* [37].

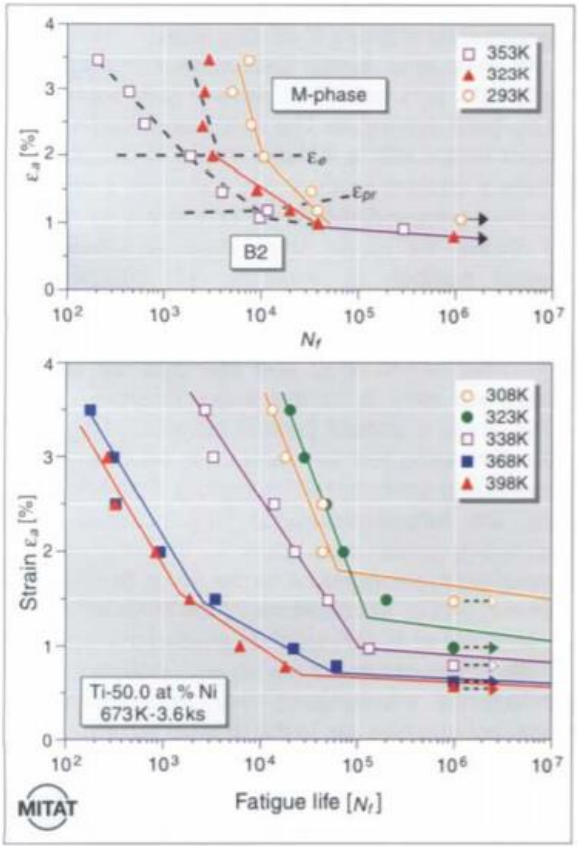

***Fig 17**. Effect of applied strain on fatigue life for Ti-50.9at%Ni (top) and Ti50.0at%Ni (bottom) alloys at various test temperatures* [37].

Nevertheless, deformation stresses need also to be considered because they affect fatigue life as well. So it is also necessary to compare the fatigue behaviour in terms of stress [37].

Fig 18. displays the stress-strain curve of a nitinol alloy. Specifically, it illustrates the proportional stress limit and the critical stress to induce the martensitic transformation.

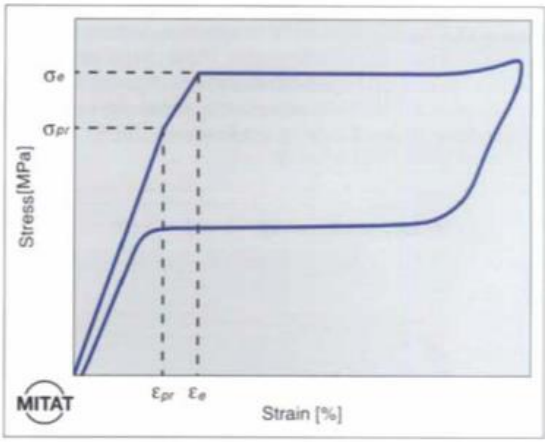

***Fig 18**. Stress-strain curve of a nitinol alloy* [37].

2.3.2.2 BIOACTIVITY OF NITINOL

The use of nitinol in applications where the material is constantly in contact with blood, as in the case of cardiovascular stents and closure devices, is problematic due its thrombogenic potential. These blood clots gradually make it difficult for blood to pass through until it is prevented, and can lead to the patient's death

Moreover, corrosion is another process extremely important to consider for the design and development of implants. The successful use of nitinol as biomaterials depends crucially on its corrosion resistance to body fluids, which are composed by ions and their corresponding biomolecules and play an important role in the corrosion effects of metals. Generally, corrosion processes, which happens in the surface of the biomaterial used as an implant as it is this zone which is in direct contact with the body fluids, are responsible for reduced biocompatibility and the emergence of undesirable reactions in implant-adjacent tissues. Corrosion is influenced by many factors such as chemical composition, surface conditions, microstructure and oxygen content, pH and temperature of the surrounding environment.

Despite the advantages of nitinol, one of the possible consequences from the corrosion of nitinol alloys is the release of Ni ions from the surface of the biomaterial. The high Ni content in the alloy is of great concern with regards to its biocompatibility because the Ni releasing is a potential danger, which could induce to toxic and allergic responses [38].

The redox reactions depend on the number of ions released into the medium (particularly Ni^{2+} ions), which is directly proportional to the amount of nickel on the surface of the material. Therefore, the preparation of the nitinol surface is essential for this material to be implantable in the human body. The formation of a layer of titanium oxide on the surface is essential for improving corrosion and

biocompatibility. This layer acts as a protective barrier against the release of Ni ions into the outer environment and surrounding tissues.

2.3.3 FUNCTIOANALIZATIONS TO IMPROVE BIOACTIVITY

In order to avoid the release of Ni ions and improve the corrosion resistance, many surface modification technologies can be used, which differ in complexity and characteristics of the surface layer formed. The effectiveness of the layer formed depends on the process of oxidation from the technique and the structure, composition, and roughness of the material.

Surface treatment techniques:

Specific coatings are required to improve the resistance to body fluid corrosion, to improve biocompatibility and reduce the release rate of Ni ions.

Physical vapor deposition (PVD): PVD coatings consist of a technique widely used in biomedical applications as it enables the modification of the surface properties of medical devices without changing the biomechanical properties of the substrate., thus improving the performance and increasing the life of medical devices [39].

Heat treatment: It consists of a technique which is performed to produce a stable oxide layer with desired mechanical properties of nitinol stents. Heat treating temperature and times for nitinol stents are chosen in the range of 450–600ºC and 10–30 min [40].

Chemical etching: The main purpose of chemical polishing is to remove impurities, defects, residual stress, and oxide films after nitinol stents are produced [40].

Electropolishing: Consists of a method which removes slag, burrs, scratches, heat-affected zones and creates a new, smoother surface. The polishing process results in a protective film consisting of pure titanium oxide [41].

2.4 ELECTROPOLISHING

Electropolishing has been used for commercial applications since the early 1950s and has evolved to become the metal finishing process of choice for parts subject to the highest standards for surface finish [8].

Among the different surface treatments which can be performed in nitinol alloys, electropolishing must be highlighted due to its great and distinctive advantages. Electropolishing is based on an anodic dissolution process in which material from a metal or an alloy is removed ion by ion from the workpiece surface. For this reason, for the implantation of coronary stents and closure devices, the electropolishing technique is widely used as it provides a smooth surface and generating a passive oxide layer on the surface improving corrosion resistance.

During this procedure, as shown in *Fig 19.,* the specimen is immersed in a temperature-controlled bath of electrolyte and serves as the anode. This part is connected to the positive polarity of a DC/AC power supply, where the negative polarity is attached to the cathode. Consequently, current passes from the anode, where metal on the surface is dissolved into the electrolyte, to the cathode. At the cathode surface, a reduction reaction occurs, in which hydrogen is normally produced. The electrolyte is normally a concentrated acid media having a high viscosity, such as phosphoric acid, sulfuric acid, and their mixtures. A schematic diagram of the experimental equipment describing all the equipment and material required is displayed in *Fig 20.*

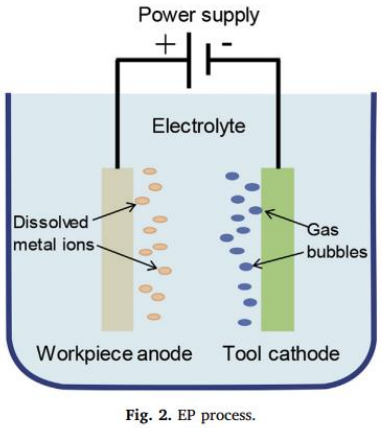

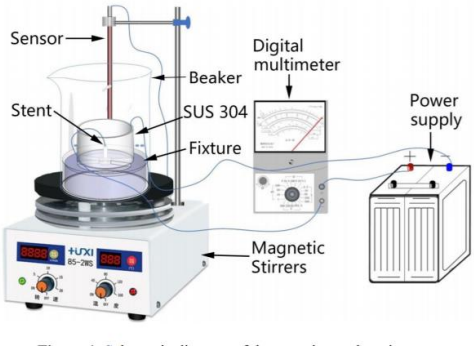

***Fig 19**. Electropolishing process* [42]**.**

***Fig 20**. Schematic diagram of the experimental equipment* [43].

2.4.1 DETERMINANT FACTORS

The EP process is influenced by many factors, including the electrolyte temperature and composition, the EP time, the initial surface roughness, the electrode rotation speed and so on [42].

-Electrolyte Temperature: Electrolyte temperature is a key factor which is directly related with the mass transport of the electropolishing process. On one hand, lower electrolyte temperatures lead to a slower diffusion of the dissolved metal/alloy ions away from the surface of the workpiece. Moreover, a reduction of the current density is also caused by low temperatures, as it decreases the solubility of metal ions in the solution.

On the other hand, with the use of higher electrolyte temperatures, the electropolishing effect is increased due to the low viscosity and a continuous supply of fresh electrolyte [42].

The higher the current density, the better the EP effect. Consequently, an increase of the electrolyte temperature causes a higher diffusive rate and a lower viscosity of the electrolyte.

-Electrolyte composition: Electrolytes used in electropolishing processes can be composed of organic, inorganic, or organic/inorganic mixtures. The main role of electrolytes is to act as carriers of the current, heat and reaction products. Depending on the type of metal to be treated, different

types of electrolytes may be used. The use of one or the other will have significant results in the result of the electropolishing process.

Typical electrolytes are composed by between a 50-75% of weight acids (being phosphoric acid and sulfuric acid mixed in a 1:1 or 2:1 ratio the most used), between a 5-15% of weight deionized water and the remaining weight corresponding to one or more inhibitors. As a result, the volume ratio of acid is of crucial importance.

-EP time: At the beginning of the EP process, the different potential distribution in the workpiece surface result in a fast-polishing effect. Moreover, as the EP increases with time, the surface becomes smoother. This effect shows the behaviour of an exponential decay of the surface roughness with time.

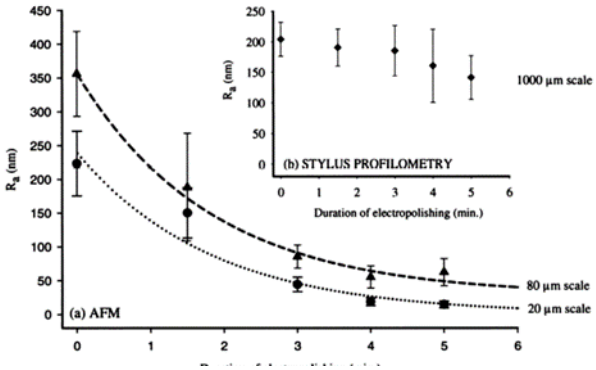

***Fig 21**. Mean roughness (Ra) vs the duration of the EP time is which the exponential decay can be appreciated* [42]**.**

-Initial surface roughness: The initial surface roughness is an important factor which influences the quality of the final electropolished surface.

Considering a profile *(see Fig 22.)* consisting of a cross-section through a surface, the horizontal lines represent the arithmetic mean height, so the total Ra corresponds to the area marked between the lines (corresponding to deviations respect to the horizontal line) divided by the total length of the profile.

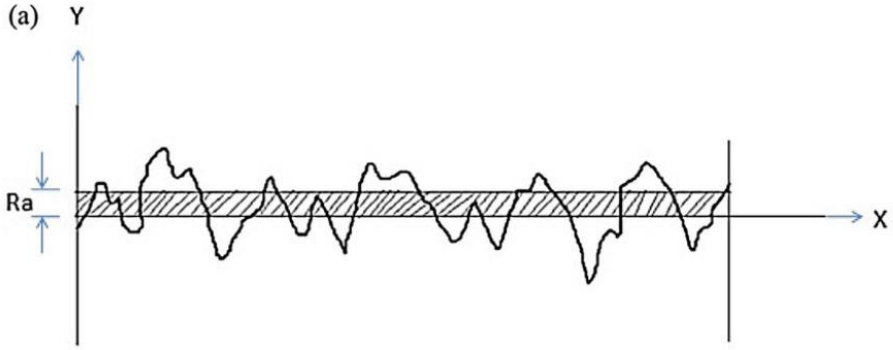

***Fig 22.** Representation of the average surface roughness (Ra)* [44].

.

EP has a limited polishing effect to improve the surface quality. Below an electropolishing process in which the Ra has been considered is described [45].

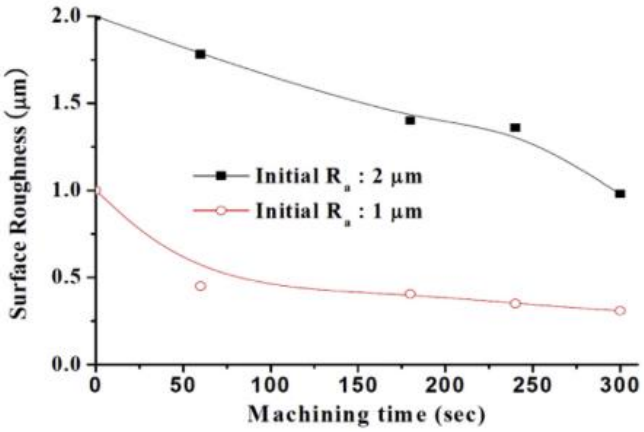

***Fig 23**. Variation of surface roughness (μm) depending on the machining time (sec)* [45].

Fig 23. shows the surface roughness variations of two different nitinol workpieces with initial surface roughness of 2 μm and 1 μm. For this experiment, an acid electrolyte composed of sulfuric acid (17.8M of H_3PO_4), phosphoric acid (14.6M of H_2S0_4) and distilled water (H_2O) was used. Moreover, the applied current was 12A, the IEG was 1mm and the machining time was 300sec [45].

The nitinol sample with an initial surface roughness of 2 μm shows a gradual improvement of Ra= 0.98 μm after 300 sec. Nevertheless, no significant improvement is seen after this period. On contrary, the nitinol sample with an initial surface of 1 μm shows a rapid improvement of Ra = 0.5 μm during a machining time of 50 sec. However, not an obvious improvement is achieved after this period.

The obtained results lead to understand that the initial surface of the workpiece should be considered carefully for a fast and effective EP process because the EP has a limitation in polishing quality [42].

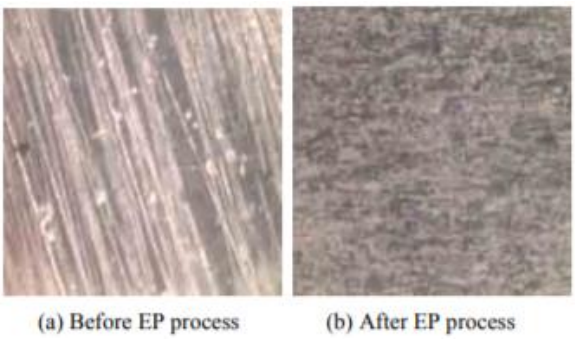

***Fig 24**. Effect of the EP process on a nitinol sample with 1 μm of initial roughness* [45].

Fig 24. shows the obtained results after an EP machining was performed on a nitinol sample with an initial roughness of 1 µm. *Fig 24. (a)* represents the surface of the sample before the EP machining whereas *Fig 24. (b)* shows the resulting surface roughness of the sample (Ra = 0.31 µm) after the EP machining was performed.

-Interelectrode gap: As the inter-electrode gap is reduced, the surface roughness of the workpiece decreases due to the higher current density. However, too narrow electrode gap causes unstable polishing and consequently, bubble marks appear on the surface. For these cases, the balance between the formation and explosion of hydrogen bubbles is broken, which result in the attachment of these bubbles on the cathode and the surface of the material.

An adequate inter-electrode gap should be selected to avoid the formation of bubble marks.

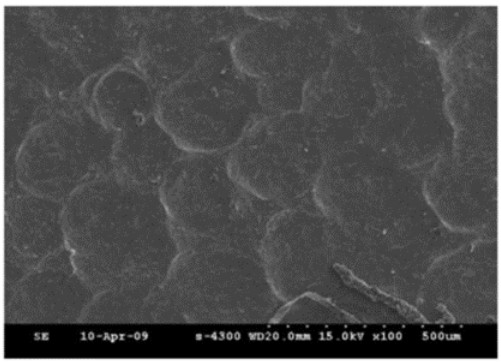

***Fig 25**. SEM image of the EP process of a nitinol shape memory alloy, in which bubble marks can be observed* [42]**.**

2.4.2 ADVANTAGES OF NITINOL ELECTROPOLISHING

As it has been explained, electropolishing technique allows the removal of surface defects as well as the smoothing of the surface with minimal material removal. Consequently, electropolished nitinol alloy is covered by a thin (about 3nm), well-defined TiO_2 layer without any free Ni ions on the surface. This ceramic layer is responsible for the outstanding corrosion resistance and biocompatibility. Electropolishing nitinol improves the alloy's resistance against corrosion as well as improves its durability by performing several different functions at once.

The main purposes for which EP process in nitinol alloys is performed are: **Finishing**, **passivation,** and **deburring**.

Finishing:

As it has been described, EP allows the smoothening and brightening of the nitinol alloy. A comparison between mechanical polishing and electropolishing of nitinol surface was carried out by W. Simka et al [46]. A surface roughness of 0.07 µm in Ra was achieved by EP whereas mechanical polishing showed a roughness of 0.18 µm in Ra.

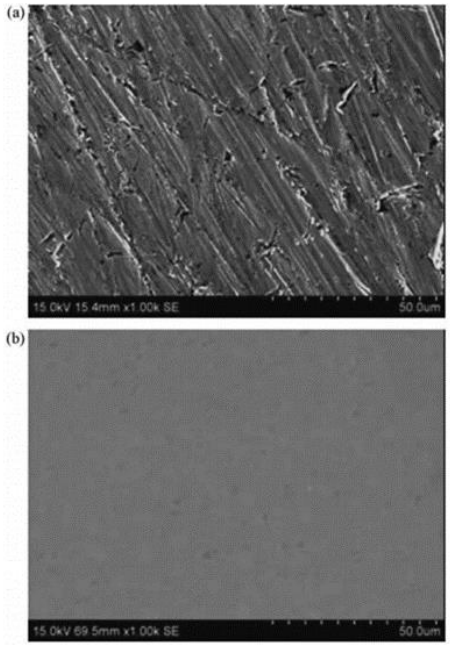

***Fig 26**. SEM images of the nitinol alloy surface of mechanical polishing (a) and electropolishing (b) samples* [46].

In order to find the optimal EP conditions, nitinols stents were electropolished at 30–40 V for 10–30s [40]. Ultimately, samples were investigated under various measurements such as scanning electron microscopy (SEM), optical microscopy (OM), atomic force microscopy (AFM). Moreover, a potentiodynamic polarization test was performed for examining corrosion behaviour.

In *Fig 27.* a SEM image of the surface quality of electropolished for 90s nitinol stents after a corrosion testing consisting of potentiodynamic polarization in NaCl solution 0.9% is displayed. Magnifications of 20x (a), 50x(b), 200x (c) and 800x(d) are displayed. As a result, no evidence of electrochemical damage was localized [47].

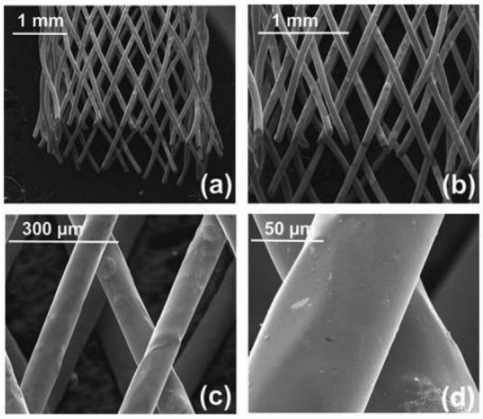

***Fig 27**. SEM images of the surface quality of electropolished nitinol stents* [47].

Electropolished coronary stents result in decreased thrombogenicity and neointimal hyperplasia after stent implantation in different animal models. The decrease of thrombus formation is most likely that EP results in a decreased surface area, resulting in less platelet adhesion and fibrinogen binding [44].

Passivation:

The concept of passivation refers to the formation of a thin layer (film) of oxide that protects the surface, since it is responsible for reducing the corrosion current values that pass through the surface of the material and consequently, decreasing the corrosion rate. The oxide layer generated is a non-reactive layer that forms on the surface of the material so that it is protected, and corrosive particles created in the implant-body interface are eliminated.

In addition to electropolishing, this oxide layer can be generated naturally by the titanium itself or by mechanical polishing. However, this last technique is less recommended since it is associated with the appearance of scratches on the surface. Other alternatives to highlight would be the coating with layers of polymers or with biological molecules. This ideal coating would be haemocompatible, thereby not inducing stent thrombosis, and could potentially reduce neointimal thickening through improved tissue compatibility [48].

An example is the case of phosphorylcholine, resulting in a reduction of thrombogenic activating [49]. Phosphorylcholine coatings are particularly effective at reducing the adhesion of a number of cell types including platelets, endothelial cells, epithelial cells, fibroblasts and macrophages [50].

Deburring:

Burrs on the components are usually generated after mechanical machining, which leads to shape deviation of the component and deteriorates its designed function. The microscopic burrs and the rough surface on nitinol alloys for medical stent makes injury on vascular, hence, it should be removed without defect of traditional mechanical machining [42].

A deburring process is necessary to provide a clean and polished surface to the stent. Therefore, micro-injuries and inflammations in the organism tissues are prevented.

Electropolishing is an optimal procedure to carry out the deburring of a metal. During this process, the transfer of metal ions occurs more quickly at the edges or corners of the sample, because in these regions the current density is higher, thus eliminating more metal at these points.

3. MARKET ANALYSIS

3.1 MARKET HISTORIC EVOLUTION

Since its discovery in 1959 by William J.Buehler, the SMA nitinol has revolutionized the production of a large multitude of devices in many engineering fields. At that time, many scientists showed special interest in this SMA and as a result, many research efforts emerged, some more successfully than others.

This little success was largely due to many problems experienced in manufacturing and developing the different devices. Problems included manufacturing difficulties (melting, processing, machining), as well as high material costs and poor availability of sources of supply.

Although nitinol was discovered in the early 1960s it was not until the 1980s that it really started to find its niche in the medical device market [19].

One of the fields of medicine that has benefited most from the excellent properties of this alloy is cardiovascular. During the 90s, these devices began to acquire great importance within the field of minimal invasive surgery. As they were relatively small devices, they could be used in considerably reduced spaces providing large deformation and relevant forces [51].

Another change to consider in recent years has been a greater understanding both from a processing technology and a device development standpoint. Moreover, special effort was put by nitinol producers to educate the industry on how to design, test and manufacture nitinol medical devices. A key element of this educational process was the formation of the Shape Memory and Super elastic Technologies Society (SMST), and the launching of its conference series starting in 1994.

Moreover, during the last two decades it has been stents and other cardiac devices that have dominated the market for biomedical instruments made with this alloy. Specifically, in 1998 the first self-expanding nitinol stents emerged, with the launch of the *Cordis SMART Stent* [52]. Its design became dominant in the marketplace and its huge success was mainly due to its very fine mesh structure that offered exceptional contouring, flexibility, and apposition characteristics [53]. It is estimated that the sale of this device around the world generated a total of 1 billion dollars, thus becoming the first product of great success in this industry.

Today, the use of devices made of nitinol has become almost a standard and is continuously growing. Two nitinol stents have been approved by the Food and Drug Administration (FDA) for use in humans: the Symphony stent (Boston Scientific) and the SMART stent (Cordis) [19]. It is estimated that the 60% of the endovascular stent market is now comprised by nitinol stents [53].

Apart from the endovascular , nitinol stents have a significant presence in other markets including urologic, upper and lower gastrointestinal, and trachea-bronchial applications [53].

3.2 FUTURE PERSPECTIVES

As explained, shape memory alloys have excellent properties which are of particular interest among many scientists when working with them. Since its discovery in 1959 by William J.Buehler, the use of SMA nitinol devices has become almost a standard and is continuously growing.

Research on new medical procedures as well as new nitinol manufacturing techniques will take place. Therefore, the market growth in medical applications will also continue [19]. It is important to highlight that, whenever surgical procedures become less invasive, nitinol-based implants will become even more important, in addition to the fact that over time their size will be considerably reduced.

Moreover, a multitude of new applications are expected to appear in the future. Some examples of future trends or emerging areas associated with this alloy would be:

- Thin film nitinol devices, as this SMA is not biodegradable, but it offers a rare combination of being robust in thin film form, and is quickly endothelialized [54].
- Porous nitinol, as the porous structure provides excellent ingrowth in living tissue and harm fixation [54].

- New and improved alloys with better mechanical and physical properties, including higher strength, radiopacity, purity and so on.

It is also important to note that in the future new methods to improve the characterization of this material will be developed. And, therefore, many of the properties offered by this alloy will be optimized, such as fatigue, durability limits and so on.

4. CONCEPTUAL ENGINEERING

As it has been already explained, this project aims to carry out an **extensive bibliographic documentation** on the properties and use of the SMA nitinol.

Moreover, it also comprises the creation of an experimental procedure to reduce the average roughness (Ra) of commercial coronary stents. This procedure will be carried out by electropolishing this nitinol cardiac devices.

There are many studies which show that electropolishing is an ideal technique to achieve a reduction of the Ra of nitinol stents. As a result, many electropolishing procedures can be performed. An extensive research has been carried out to select the optimum conditions on electropolishing.

4.1 STUDY OF SOLUTIONS

This section presents 4 different scientific studies in which electropolishing has been performed. Each of them uses different electrolytes and different experimental procedures. The different conditions used in each procedure are described, as well as the results obtained.

4.1.1 ELECTROPOLISHING IN METHANOLIC H_2S0_4

H_2S0_4 can be used as an electrolyte to stablish and study the conditions for electropolishing of titanium. According to *K.Fushimi et al* [55], anodic polarization of nitinol up to 8 V was performed in various aqueous and methanolic H_2S0_4 solutions. The dissolution kinetics depends on the polarization potential, the H_2S0_4 concentration, the water concentration, and the temperature.

With a concentration of H_2S0_4 in solutions varying from 0.1 to 7 mol dm^{-3}, best results were obtained for a 3 mol dm−3 methanolic H_2S0_4 at 263K. A smooth mirror like surface was given and this result showed a potential independent limiting current in a wide potential range [55].

For concentrations up to 0.3 mol dm^{-3}, no electropolishing conditions were observed, showing a linear increase of current with potential.

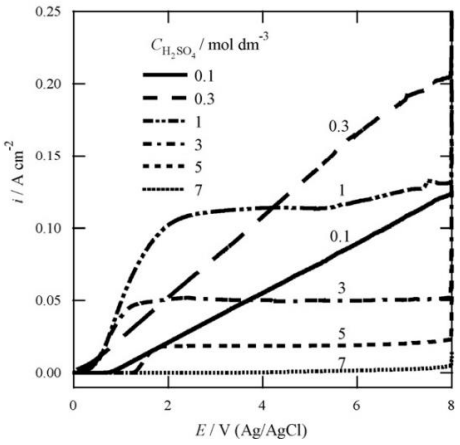

***Fig 28**. Anodic polarization curves of nitinol in 0.1 to 7 moldm-3 H2S04 solutions* [55].

For concentrations equal to1 mol dm^{-3} or higher, the current increases until a plateau region is achieved, which is practically independent on the potential.

Moreover, larger concentrations of H2SO4 (5-7 mol dm^{-3}), result in a decrease in the limiting current.

4.1.2 ELECTROPOLISHING USING n-BUTANOL and NITRIC ACID

Study carried out by J.Kim et al [40], presents the optimal electropolishing conditions for nitinol stents, specially focusing of the EP voltage and time. Electropolishing conditions for this study were: EP performed at room temperature with different parameters, voltage: 30, 35, 40 V and time: 10, 20, and 30 s. Finally, current density and electrode distance were fixed at 50 mA and 50 mm, respectively. Moreover, heat-treatment was also performed which clearly numerous defects and pits on the surface samples, demonstrating that EP is a necessary process in the manufacturing of nitinol stents.

After EP was performed, nitinol stents were investigated under various measurements such as scanning electron microscopy (SEM), optical microscopy (OM), atomic force microscopy (AFM).

Best results were obtained by performing EP under 40 V-10 s. A smooth and uniform surface with a roughness **Ra = 22.29 nm** was obtained.

4.1.3 ELECTROPOLISHING USING ETHYLENE GLYCOL-NaCl

In this study [43], surface integrity of cardiovascular stents fabricated with nitinol alloy was tested by adding distilled water of different concentration into ethylene glycol - sodium chloride electrolyte [43]. To determine the optimal electropolishing conditions, I-V curves and surface roughness were measured.

After performing various experiments under different conditions, it was possible to determine the optimal conditions with which a significant improvement in the surface integrity of the cardiovascular stents was achieved. The best results were obtained with a concentration of the electrolyte ethylene glycol-NaCl of 1mol/L, with a concentration of distilled water of 1 vol.%. Moreover, the optimal polishing voltage was 17.5 V, with a polishing time of 15m.

Under these conditions, the best results were obtained in terms of the average roughness of nitinol stents, with a value of **Ra=78.4 nm** and a material removal rate of 2 μm/min [43].

4.1.4 ELECTROPOLISHING USING ACETIC AND PERCHLORIC ACID

In this study, E. Kassab et al [47], for the electropolishing of nitinol stents, a mixture of 79 vol.-% of acetic acid and a 21 vol.-% of perchloric acid electrolyte was used. Electrolyte was maintained at 20 ± 1 °C and subjected to a 10V potential. Electropolishing time varied from 15s to 120 s. After electropolishing was performed, stents were rinsed with distilled water, ultrasonically cleaned in ethyl alcohol, and dried.

Fig 29. shows the nitinol surface of stents after electropolishing technique was performed at varying polishing times (15s-125s). It could be concluded that best surface quality of stents was obtained by increasing polishing time to 75 s and 90s. Longer times (105-125s) show clearly a non-uniform loss of material as well as pit formation.

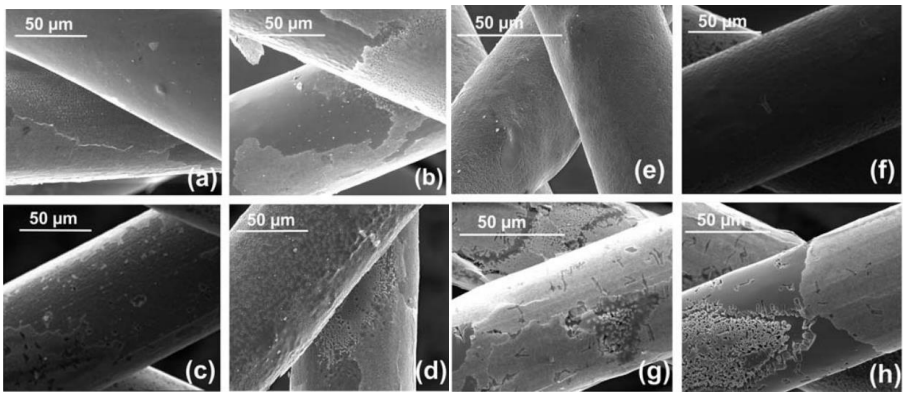

***Fig 29**. SEM images of nitinol stents after electropolishing time of (a) 15s,(b) 30s, (c) 45s, (d) 60s, (e) 75s, (f) 90s (g) 105s ,(h) 125s* [47].

Moreover, potentiodynamic tests results confirmed the improvement of the surface quality, regarding corrosion resistance after electropolishing. *Fig 30.* displays the surface quality of non-electropolished stents and electropolished stents after a potentiodynamic polarization in NaCl solution 0.9% was carried out. As a result, no evidence of localized electrochemical attack was detected on the surfaces of the EP samples.

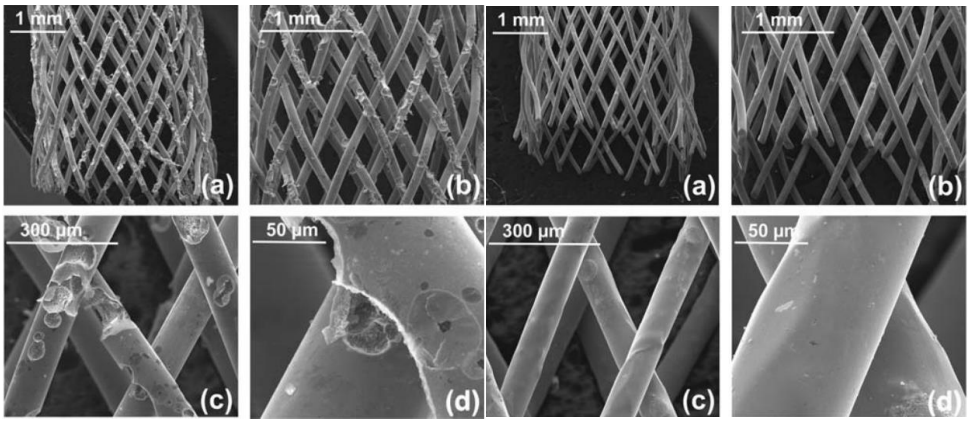

***Fig 30**. Comparison between non-electropolished stents (left) and electropolished stents (right) after potentiodynamic polarization in NaCl solution 0.9%* [47].

4.2 PROPOSED SOLUTION

After performing a detailed study among all the electropolishing procedures described in the previous section, electropolishing by using ethylene glycol - sodium chloride electrolyte was considered as the most optimal.

The rest of the electrolytes proposed in the previous studies were discarded. The reason of it was because they were acidic electrolytes. Their use represents a much more complicated process, a higher economic cost, in addition to the higher risks associated when working with this type of electrolytes. Due to these factors, ethylene glycol - sodium chloride electrolyte was chosen as the most viable option to perform EP processes.

The conditions used to develop the experiment were based on the study previously explained in section 4.1.3 [43]. As it was demonstrated, the use of this electrolyte for electropolishing nitinol stents proved to be highly effective in improving the surface quality of the samples. Average roughness (Ra) values of 78.4nm were achieved.

The most optimal conditions of this study were used as a basis, with an EP time of 15 minutes, an applied voltage of 17,5V, a concentration of the electrolyte ethylene glycol-NaCl of 1mol/L, with a concentration of distilled water of 1 vol.%.

Moreover, parameters such as temperature, voltage or EP time were varied so that a wide range of conditions could be studied and, consequently meet one of the main objectives: Selecting the most optimum conditions on electropolishing process.

5. DETAILED ENGINEERING

This section explains in detail the protocol followed for the development of the project's experimental part. This process includes from the preparation of the samples to the interpretation and evaluation of the results obtained.

5.1 EXPERIMENTAL PROCEDURE

5.1.1 SAMPLE PREPARATION

The study was performed using samples consisting of commercial nitinol stents with a length of 0.32mm. These samples were provided by a company specialized in manufacturing nitinol-based cardiac devices, so no cost was associated to the material acquisition. *Fig 31.* shows the nitinol samples used to carry out the experiment.

Due to the scarcity of samples and considering the amount of electropolishing process under different conditions to be performed, it was necessary to separate each of the samples into tiny pieces. As a result, from a single cardiac device, about 10 samples could be obtained.

***Fig 31**. Entire nitinol sample used.*

5.1.1.1 Cleaning protocol

Before starting with the electropolishing procedure it was necessary to carry out a cleaning process. The aim of it was to ensure that there was no contamination on the surface of the samples, either fat or dirt that could potentially affect the samples.

To perform this process, the samples were placed in a magnetic stirrer for 5 minutes, inside a beaker with milli-Q water, along with **sodium dodecylbenzenesulfonate** (CAS: 25155-30-0) (a compound used as a detergent). Once this process was finished, the samples were transferred to another beaker with milli-Q water and were subjected to a total of 3 cycles of ultrasound. Each of these rinsing cycles lasted 5 minutes and allowed to remove any type of impurity that had been present from the previous cleaning.

Once the 3 cycles were finished, the samples were ready to be electropolished.

5.1.2 ELECTROLYTE PREPARATION

The next procedure to be performed was the preparation of the electrolyte. As previously explained, ethylene glycol – sodium chloride electrolyte was used. To perform this procedure, the concentration of distilled water required was 1 vol.%. A total amount of 100ml of electrolyte was prepared, so 99ml of ethylene glycol (CAS: 107-21-1) were mixed along with 1ml of milli-Q water.

On the other hand, as NaCl concentration had to be 1mol/L, the calculation of the total grams of NaCl was carried out. Specifically, it was necessary to introduce 5.84 g of NaCl which were calculated with precision and accuracy with the help of a scale.

5.1.3 ELECTROPOLISHING

To perform the electropolishing process of the samples, different components were required. *Fig 32.* shows all the necessary equipment used for the electropolishing processes.

***Fig 32**. Electropolishing equipment used.*

To perform this procedure a copper sample was used as a cathode, which was connected to the negative pole of the source of electric current. On the other hand, the positive pole of the current source was connected to the samples to be electropolished, acting as the anode.

Moreover, it was important that the sample could rotate constantly during the whole electropolishing process. The reason for this circular movement was to try to achieve a completely homogeneous polishing, reducing as much as possible the concentration of species on the surface.

Finally, it should be noted that a thermometer was required to measure the temperature of the electrolyte during polishing. This thermometer is of vital importance, since it allows to know the

temperature at which the experiment is being carried out, and as previously explained, it is a determining factor of electropolishing.

5.2 CHARACTERIZATION

Once the electropolishing process was finished, each of the samples was stored individually and labelled according to the day it was prepared and the EP conditions used. Then, the characterization of the polished samples was carried out. This procedure allowed to obtain the corresponding images of the samples and thus be able to study the surface quality achieved, in addition to the roughness parameters.

5.2.1 CONFOCAL MICROSCOPY

The confocal microscope was used to obtain all the necessary images to later study in detail the surface quality of the samples.

This type of microscope uses a laser as a source of light that passes through a filter with a hole. Its main advantage over the conventional optical microscope is its ability to illuminate the specimen point by point, also eliminating light from unwanted planes.

By using this microscope, it was possible to determine the topography of the samples as well as the roughness measurements. Specifically, the microscope used was the *Sensofar* and the software *SensoSCAN 2300* was used to obtain the images.

In addition, the EPI 150X lens was used and a bottom-to-top sweep was performed in an area of 56.52 x 56.52 µm2.

5.2.2 SCANNING ELECTRON MICROSCOPY AND FIELD EMISSION SCANNING ELECTRON MICROSCOPY

Another of the characterization techniques that was used was the scanning electron microscopy (SEM). This microscope allows to study the composition of the samples as well as their morphology. The *Jeol 5310* microscope was used, with a potential of 20Kv, and the samples were imaged with different magnification 2500x, 5000x to be able to study the electropolished regions with greater detail.

Moreover, the Field Emission Scanning Electron Microscope (FESEM) was used as well to obtain quality images and therefore characterize the samples.

5.3 IMAGE PROCESSING WITH GWYDDION SOFTWARE

The Gwyddion program is a Free and open-source software for SPM (scanning probe microscopy) data visualization and analysis. This software is intended for the analysis of height fields obtained by SPM techniques.

Once the images of the confocal microscope were acquired, this software was used to process them, study the surface quality of the samples, and extract the corresponding roughness parameters. It is important to mention that, to make data the most significant, 5 different roughness measurements were taken for each of the samples. Then, arithmetic mean and standard deviation was assessed.

To process each of the images it was necessary to follow a specific protocol. However, due to its length extension, it has been decided to incorporate the explanation of this protocol in the annexes section.

5.4 RESULTS

5.4.1 EXCEL DATA PROCESSING

Once the roughness parameters were extracted, Excel software was used to process all data. As explained, each sample had 5 different roughness measurements, so the program was used to calculate the arithmetic mean and standard deviation.

Gwyddion software allows to extract a wide variety of roughness parameters, as seen in *Table. 3.* Among all of them, the average roughness (Ra) was chosen as the parameter to compare between the samples.

Roughness parameters	
Cut-off:	8,84847
Roughness average (Ra):	1,83966
Root mean square roughness (Rq):	2,503284
Maximum height of the roughness (Rt):	16,83418
Maximum roughness valley depth (Rv):	8,542252
Maximum roughness peak height (Rp):	8,291952
Average maximum height of the roughness (Rtm):	10,461666

***Table. 3**. Excel data processing of roughness parameters.*

Roughness parameters represented in correspond to the nitinol sample without electropolishing. Once the mean and standard deviation was performed, the average roughness obtained was **Ra = 1,83µm ± 0,1306.** Consequently, this value will be compared with the results of the other samples. This will allow determine whether electropolishing is an effective method or not to reduce the average roughness of the samples.

Once the Ra arithmetic mean of each sample was assessed, the interpretation of results was carried out.

5.4.2 RESULTS ASSESSMENT

This section presents the results obtained during the experimental procedure.

Different conditions of voltage, polishing time and temperature have been used, always using the same electrolyte. Therefore, one of these parameters was modified while the other two remained constant. This section is divided into 3 parts:

5.4.2.1 TEMPERATURE VARIATION EFFECT

To study the effect of temperature, a set of samples were electropolished keeping the polishing time and voltage parameters constant. EP polishing time of 10 minutes and a voltage of 17,5 V were established.

Two images corresponding to one of the samples processed in this section are displayed below. *Fig 33.* corresponds to the 3D view obtained using the confocal microscope, whereas *Fig 34.* on the right was obtained using the Field Emission Scanning Electron Microscopy (FESEM). This sample was electropolished at **22ºC for 10' at 17,5V** (sample reference 22ºC_10'_17,5V).

CONFOCAL

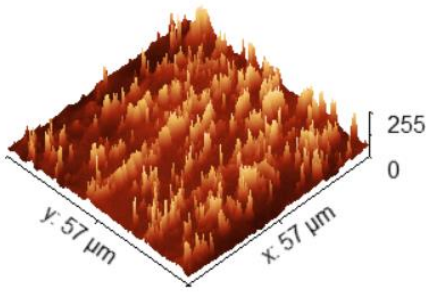

***Fig 33**. 3D view of the 22ºC_10'_17,5V sample.*

FESEM

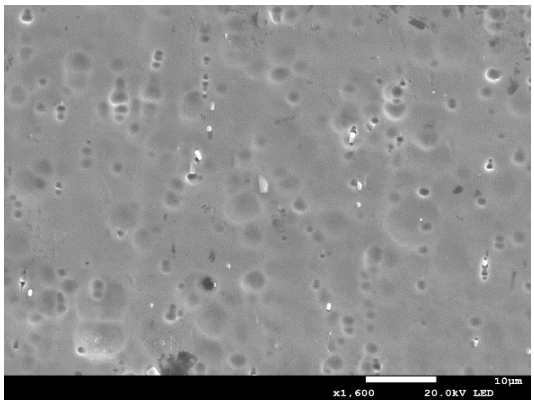

***Fig 34**. FESEM image of the 22ºC_10'_17,5V sample.*

The results obtained for the different temperature conditions at 22, 28 and 29ºC were compared, as shown in *Table. 4.*

Temperature (ºC)	Voltage (V)	Time (minutes)	Ra (nm)
22	17,5	10	99,8655 ± 8,3475
28			173,4256 ± 22,4399
29			167,3807 ± 50,2683

Table. 4. *Roughness values Ra at 22, 28 and 29 º C, applying a voltage of 17, 5 V for 10 minutes.*

Moreover, a graphical representation of the Ra values according to the temperature used has been added (see *Fig 35.*).

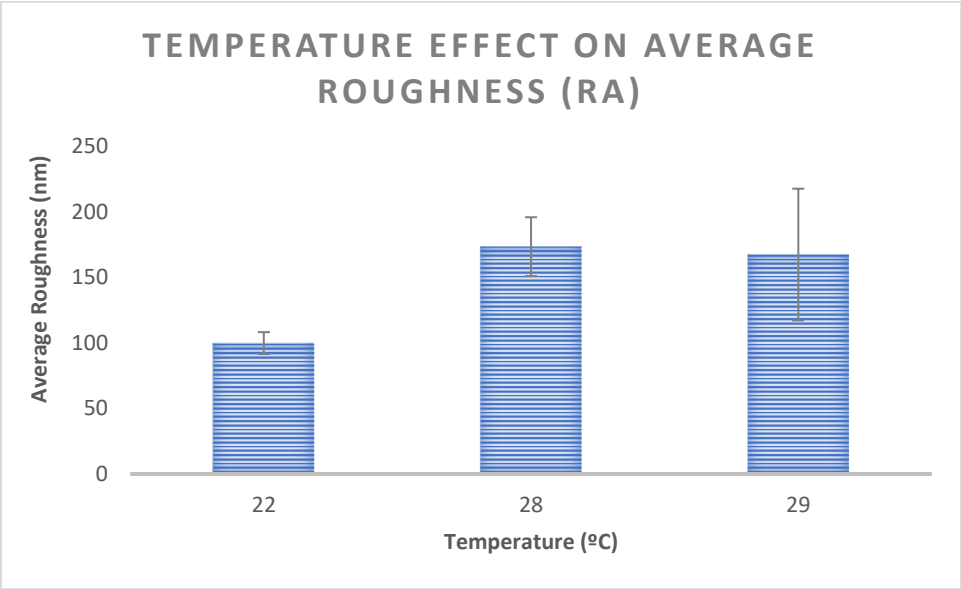

Fig 35*. Temperature effect on average roughness (Ra) values.*

The lowest value of Ra is obtained at **22ºC** with **Ra= 99,8655 nm ± 8,3475**. The difference in terms of Ra in 28 and 29 degrees is not very perceptible. This is probably because there is only one-degree (ºC) of difference between the two samples.

To analyse how temperature has significantly affected the results, the percentage difference of Ra between the cases of 22 and 28 degrees has been assessed. (see *Table. 5.).*

Temperature (ºC)	Ra (nm)	Difference (%)
22	99,8655	42,4 %
28	173,4256	

Table. 5. *Ra values for each temperature and percentage difference.*

Using a temperature of 22ºC has meant a reduction of **42.4%** of the Ra with respect to a 28ºC temperature.

Therefore, it can be determined that at high temperatures (28-29ºC) the products generated by oxidation are not being properly eliminated. As a result, these are increasing the final roughness of the sample.

5.4.2.2 VOLTAGE VARIATION EFFECT

To study how the voltage affected, a constant temperature of 22ºC was maintained. In addition, to increase the number of conditions, two different polishing times (10 and 5 minutes) were used. The voltages applied were 22,5 V and 17,5V.

As before, two confocal and FESEM images are displayed below, corresponding to the samples electropolished in this section. First two images correspond to the sample electropolished at **22,5V for 10 minutes at 22ºC.**

CONFOCAL

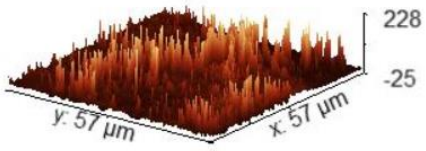

***Fig 36**. 3D view of the 22ºC_10'_22,5V sample.*

FESEM

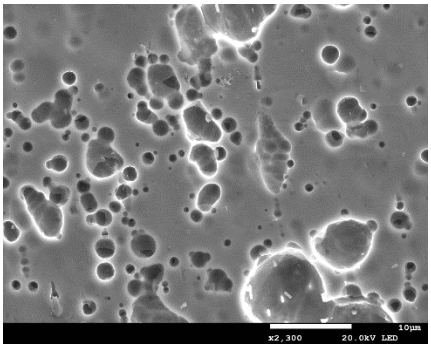

***Fig 37**. FESEM image of the 22ºC_10'_22,5V sample.*

Next two figures (*Fig 38., Fig 39.*) correspond to the sample electropolished at **17,5V for 5 minutes at 22ºC.**

CONFOCAL

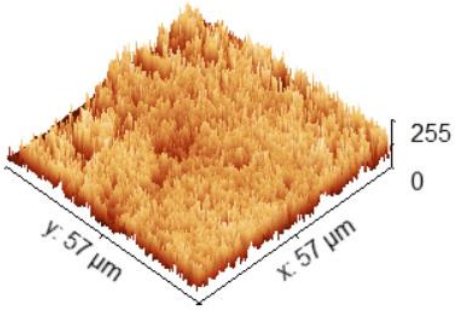

***Fig 38.** 3D view of the 22ºC_5'_17,5V sample.*

FESEM

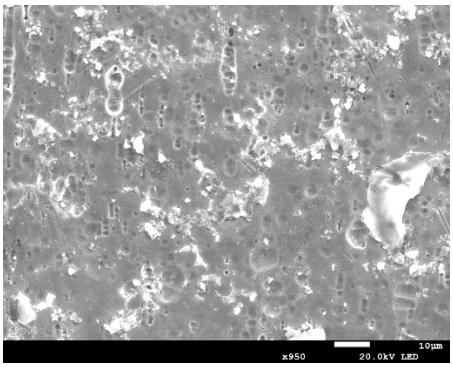

***Fig 39**. FESEM image of the 22ºC_5'_17,5V sample.*

The conditions used to study how voltage affected the EP process are described in *Table.6*. Ra values as well as their standard deviation are also included.

Temperature (ºC)	Voltage (V)	Time (minutes)	Ra (nm)
22	17,5	5	48,37845 ± 17,7898
		10	99,865525 ± 8,3475
	22,5	5	47,821283 ± 19,4495
		10	83,5851 ± 26,4317

Table. 6. *Roughness values Ra at 22 °C by applying voltages of 22, 5 and 17.5 V for 5 and 10 minutes.*

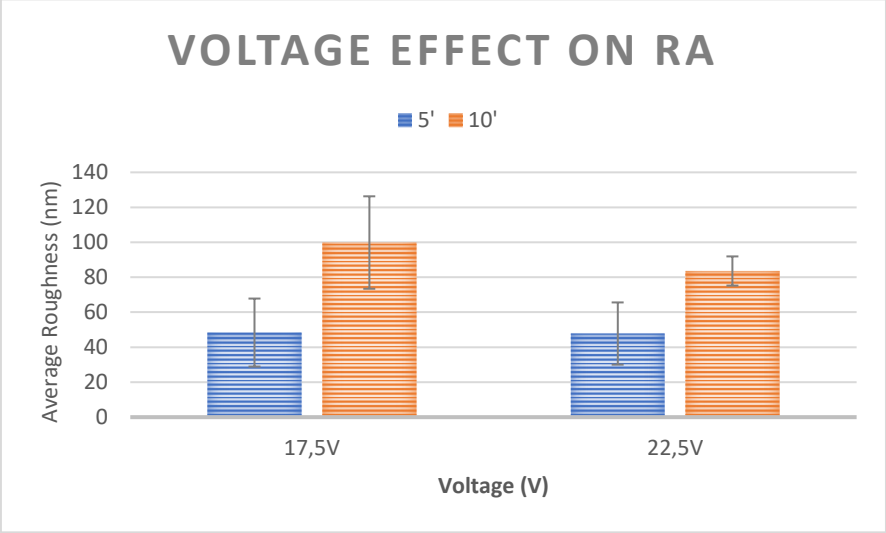

Fig 40. *Voltage effect on Ra at different times.*

Fig 40. represents the voltage effect on the average roughness (Ra). As it can be clearly identified, Ra values decrease as a higher voltage is applied.

In this section it has also been calculated the percentage difference between the samples electropolished for 5 minutes applying 17,5 and 22,5 V. The same procedure has also been performed for the 10-minute samples. In this way, it can be studied how voltage affected the EP process.

Voltage (V)	EP time (min)	Ra (nm)	Difference (%)
17,5	5	48,37845 ± 17,7898	1,15%
22,5	5	47,821283 ± 19,4495	
17,5	10	99,865525 ± 8,3475	16,3%
22,5	10	83,5851 ± 26,4317	

***Table. 7**. Mean Ra for each voltage and percentage difference.*

As it is displayed in *Table. 7.*, the percentage difference between the two samples electropolished for 5 minutes each at different voltages is **1.15%.** Therefore, it makes a very small difference.

On the other hand, the percentage difference between the two samples electropolished during 10 minutes at different voltages is **16,3%,** a much bigger difference than the previous one.

These percentage differences led to understand that time is a very important factor in the electropolishing process. Next up, an analysis on how this parameter affects is performed.

5.4.2.3 EP TIME VARIATION EFFECT

Finally, how affected the polishing time was studied as well. Therefore, the two cases described previously were analysed, now comparing the EP times.

- On one hand, at 22,5 V, EP times of **10** and **5** minutes were stablished.
- On the other hand, polishing times of **10** and **5** minutes were used at 17,5V.

Temperature (ºC)	Voltage (V)	Time (minutes)	Ra (nm)
22	17,5	5	48,37845 ± 17,7898
		10	99,865525 ± 8,3475
	22,5	5	47,821283 ± 19,4495
		10	83,5851 ± 26,4317

***Table. 8.** Roughness values Ra at 22 º C applying voltages of 22,5 and 17,5V for different times.*

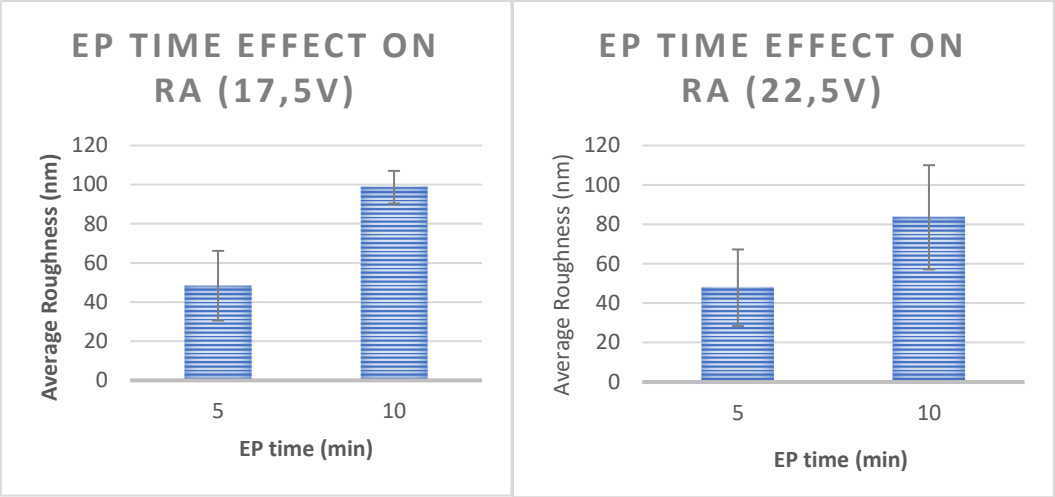

***Fig 41**. a) EP time effect on Ra for 5 and 10' at 17,5 V, (b) EP time effect on Ra for 5 and 10' at 22,5V.*

As seen in *Fig 41.*, EP time is also a determining factor to consider. As this time increases, the average roughness of the samples increases as well.

This event happens for both cases using voltages of 22.5 and 17.5 V, respectively.

- Applying 17.5V also shows a clear difference in the decrease of Ra, dropping from 99,8655 nm in 10 minutes to 48,3784 in 5 minutes. The percentage difference in Ra between both times is **51,6%.**

EP time (min)	*Ra (nm)*	***Difference (%)***
5	48,37845 ± 17,7898	**51,6%**
10	99,865525 ± 8,3475	

***Table. 9**. Roughness values Ra applying 17,5V for 10 and 5 minutes and percentage difference.*

- Applying 22.5V, the minimum value of Ra was achieved by setting a EP time of 5 minutes with Ra = **47.8212 nm**. The percentage difference of Ra between the EP samples at 10 and 7 minutes is **46.41%.**

EP time (min)	*Ra (nm)*	***Difference (%)***
5	47,821283 ± 19,4495	**42,8%.**
10	83,5851 ± 26,4317	

***Table. 10**. Roughness values Ra applying 22,5V for 10 and 7 minutes and percentage difference.*

Both results (*see Table.9.*, *Table.10.*) demonstrate how EP time significantly affects the Ra of the samples.

So far has been analysed how the factors of EP time, voltage and temperature affect the Ra values. It is now possible to determine, from among all cases, the minimum value of Ra obtained.

As analysed, the lowest Ra value obtained was **47,821283 nm ± 19,4495**. Therefore, most optimum conditions on electropolished process were found by stablishing a temperature of 22ºC applying 22.5V for a duration of 5 minutes.

Taking into account that the Ra of the original sample without electropolishing was **1,83µm ± 0,1306,** the percentage difference between the two samples can be calculated. As a result, it can be determined that the electropolishing process under the most optimal conditions has achieved a reduction in Ra of **97.4%.**

It should also be noted that with other conditions excellent results were achieved in terms of Ra reduction. It has been determined that increasing the voltage, reducing the EP time, and working at room temperature (approximately 22º) has considerably favoured the reduction of average roughness of the samples.

6. CHRONOGRAM PREVISION

6.1. WBS AND WBS DICTIONARY

In order to guarantee the success of a project, it is essential that its management is as optimal and adequate as possible. A tool that is of vital importance for project management, regardless of the size of this, is the **WBS** or work breakdown structure.

It is a graph that exposes in a schematic way the different stages of the project, as well as all the tasks to be performed in each of them. It allows to divide the different work packages according to the relationship between the tasks and clearly visualize the structure of the project. The WBS of this project is outlined below. (*see Fig 41.).*

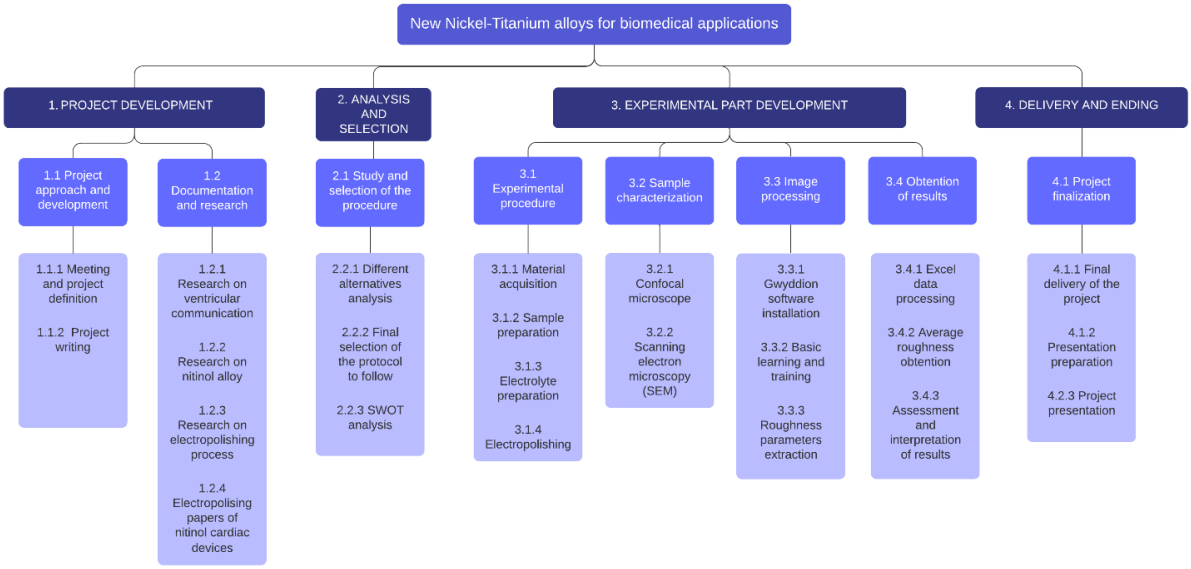

***Fig 42**. WBS of the project*

This section also includes the WBS dictionary, which describes in detail each of the phases and tasks of the Project.

1. **PROJECT DEVELOPMENT:** The first section of the project refers to its own development. It includes the selection of the project's topic, the writing of the project as well as all the tasks of bibliography and documentation.

2. **ANALYSIS AND SELECTION**: Once an extensive documentation has been made on the different topics included in the project, all the alternatives relating to the experimental part will be analysed in detail and the option that is most viable will be selected to be implemented in the laboratory.

3. **EXPERIMENTAL DEVELOPMENT**: This stage of the project refers to the experimental part that is developed in the laboratory. These include tasks relating to the experimental procedure, the process of characterizing the samples, the processing of the images and the obtaining and interpretation of the results.

4. **DELIVERY AND ENDING:** This last stage corresponds to the completion of the writing of the project and the delivery of the same. Moreover, it also includes the preparation of the presentation and its subsequent presentation.

6.2. PRECENDE ANALYSIS

To identify more easily the different tasks of the project, *Table. 11.* has been created, which relates each project task to a letter and its identification number that also appears in the WBS. In addition,

the precedence of each of the activities has also been analysed.The precedence analysis has allowed to create the PERT diagram that will be explained later in more detail.

EDT REFERENCE	TASK	TASK CODE	PRECEDENCE
1.1.1	Meeting and project definition	A	-
1.1.2	Project writing	B	A, C,D,E,F,U
1.2.1	Research on ventricular communication	C	A
1.2.2	Research on nitinol alloy	D	A
1.2.3	Research on electropolishing process	E	A
1.2.4	Papers on electropolishing nitinol cardiac devices	F	D, E
2.1.1	Analysis of the different alternatives	G	F
2.1.2	Final selection of the protocol to follow	H	G
2.1.3	SWOT analysis	I	H
3.1.1	Material acquisition	J	G,H
3.1.2	Sample preparation	K	H,J
3.1.3	Electrolyte preparation	L	H,J
3.1.4	Electropolishing	M	K,L

3.2.1	Confocal microscopy	N	M
3.2.3	Scanning electron microscopy and FESEM	O	M
3.3.1	Gwyddion software installation	P	A
3.3.2	Basic program learning and training	Q	P
3.3.3	Roughness parameters extraction	R	N,Q
3.4.1	Excel data processing	S	R
3.4.2	Average roughness obtention	T	S
3.4.3	Assessment and interpretation of results	U	T
4.1.1	Final delivery of the project	V	B,U
4.1.2	Presentation preparation	W	U
4.1.3	Project presentation	X	V

***Table. 11**. Codes assigned together with their reference in the WSD and the precedence among tasks.*

6.3 DEFINITION OF TASKS AND TIMES

This section presents in detail the development of the project over time, as well as the different tasks have been happening from the moment in which the present work began until its subsequent completion and presentation.

6.3.1 DEFINITION OF TIMES

The present project has had an approximate duration of about 8 months. Specifically, it began during the first week of November 2020, when the topic of the project was selected, and concluded with its presentation in June 2021.

During the first 4 months, the time was committed to an extensive literature and research focused on different areas. These include from information about nitinol alloy and its potential biomedical applications, to cardiovascular pathologies that could be treated with nitinol-based implants. During this period, techniques to improve the biocompatibility of these devices as well as different electropolishing studies of nitinol samples were also analysed.

Once this research literature was completed, the different alternatives were studied in detail together with the project tutor with the aim of deciding which of the different options should be chosen as the object of study.

During the month of April 2021, the experimental part of the project began in the laboratory. First assays took long time to be carried out until arriving to the point of getting familiar with the steps to follow. As a result, it was a matter of time to feel more confident in the laboratory environment.

During this month and the middle of May, the different electropolishing procedures were carried out. Moreover, the confocal microscope was also used to acquire images of the samples to be processed later.

As for the image processing part, as explained, it was necessary to install and learn how to use the Gwyddion software (protocol explained in annexes section). In order to optimize the time, this software was installed at the same time that the electropolishing processes were carried out, so that, once the samples were ready and the images obtained, the software would already be installed and ready to be used.

Finally, during the second half of May, all the processing of the images obtained by means of the confocal microscope was carried out. In addition, the processing of data using the Microsoft Excel software was performed to determine the average roughness of the samples. Once a proper data processing was carried out, it was possible to determine the optimum EP conditions.

It is also important to clarify that the process of writing the project has been carried out throughout this period, since the beginning of the research literature and parallel to the experimental part carried out in the laboratory.

6.3.1.1 TOTAL TIME ESTIMATION

To estimate the time available to carry out the project, the beta distribution equation (*see Equation 1*) was used. It includes three different time durations which have been determined subjectively:

-An optimistic duration **(OP)**

-A pessimistic duration **(PES)**

-A more likely duration **(PROB)**

Beta distribution formula consists of a weighted average in which more weight is given to the most likely estimate. As a result, it has been possible to calculate the expected duration of each of the activities and the total duration of the project. It should be added that durations are expressed in units of time corresponding to days.

$$ESTIMATED = \frac{Optimistic + 4(Probable) + Pessimistic}{6}$$

Equation 1. Beta distribution formula

ACTIVITY CODE	OP	PROB	PES	ESTIMATED
A	2,5	3	5	3,25
B	45	60	80	60,83
C	8	14	21	14,16
D	12	14	16	14
E	10	12	15	12,16
F	16	18	24	18,66
G	2	4	6	4
H	1	2	3	2
I	2	3	4	3
J	18	25	30	24,66
K	5	8	10	7,83
L	1	2	2	1,83
M	15	26	35	25,66
N	10	15	23	15,5
O	1	1	2	1,16
P	1	2	2	1,83
Q	2	3	4	3
R	4	6	8	6
S	20	25	30	25
T	5	6	7	6
U	8	12	16	12
V	1	1	1	1
W	4	7	12	7,33
X	1	1	1	1
	194,5	270	357	271,91

***Table. 12**. Definition of the optimistic, pessimistic, probable and expected times of each project task.*

6.3.2 DEFINITION OF TASKS

Table.13. displays the assignment of the tasks to be developed during the project. As it can be appreciated, only one person was in charge of performing all tasks. However, it is important to mention that the tutor's supervision was always counted on.

TASK	RESPONSIBILITY
Project Development	**CARLES GARÍ CRESPÍ (biomedical engineer)**
Experimental procedure	
Sample Characterization	
Data processing and results	

***Table. 13**. Assignment of the main tasks to be developed in the project.*

6.4 CRITICAL PATH ANALYSIS AND PERT

From the precedence matrix it has been possible to create the PERT graph. In addition, the critical path that informs the minimum time in which the project can be developed has also been determined.

Therefore, below, this PERT chart is shown (*see Fig 42.)* with its critical path marked in purple.

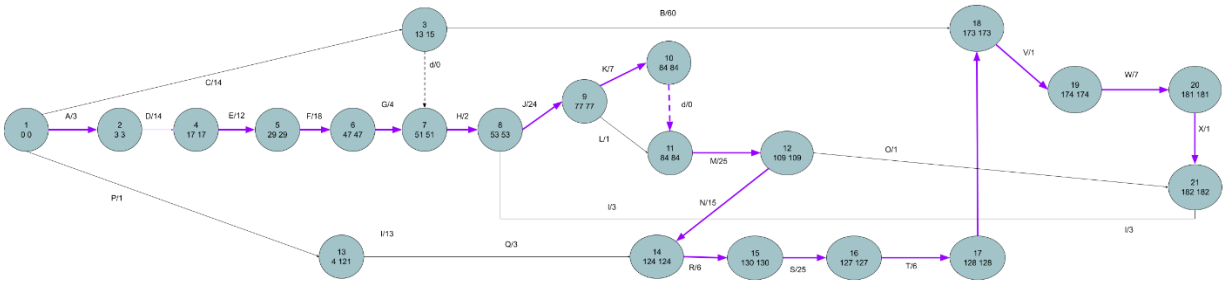

***Fig 43.** PERT chart.*

Once this diagram has been made, it has been observed that the minimum time in which the project can be developed is **182 units of time**, which is equivalent to days. Due to the extension limit of the project, a reduced diagram is incorporated in this section. However, in the annexes section, the augmented PERT diagram is included.

6.5. GANTT CHART

This section includes the GANTT chart, an important tool in the development of a project, since it allows to visualize how the tasks have been temporarily distributed throughout the development of the project. It establishes the division of working time and expresses the passage of time in a linear way from the beginning to the end of the project. It is possible to appreciate graphically how much time will be allocated to each activity. Moreover, informs of which of these can be carried out simultaneously, since it shows the interdependence between the different tasks.

Tasks	Start Date	Due Date
1. PROJECT DEVELOPMENT	11/02/20	06/21/21
1.1 Project approach and development		
Meeting and project definition	11/01/20	11/01/20
Project writing	06/06/21	06/13/21
1.2 Documentation and research		
Research on ventricular communicat	11/09/20	11/18/20
Research on nitinol alloys	11/25/20	01/21/21
Researchon electropolishing process	12/14/20	01/28/21
Nitinol cardiac devices electropolishi	02/02/21	03/10/21
2 ANALYSIS AND SELECTION	03/15/21	03/29/21
2.1 Different alternatives analysis	03/15/21	03/22/21
2.2 Final selection of the protocol	03/24/21	03/25/21
2.3 SWOT analysis	03/29/21	03/29/21
3 EXPERIMENTAL PART DEVELOPMENT	03/31/21	06/04/21
3.1 Experimental procedure	03/31/21	05/14/21
Material acquisition	03/31/21	04/09/21
Sample preparation	04/12/21	04/16/21
Electrolyte preparation	04/19/21	04/22/21
Electropolishing	04/27/21	05/14/21
3.2 Sample characterization	05/04/21	05/18/21
Confocal microscope	05/05/21	05/18/21
Field Emission Scanning Microscope	05/14/21	05/14/21
3.3 Image processing	05/19/21	05/31/21
Gwyddion software installation	05/12/21	05/12/21
Basic learning and training	05/19/21	05/21/21
Roughness parameters extraction	05/21/21	05/25/21
3.4 Obtention of results	05/25/21	06/04/21
Excel data processing	05/25/21	05/29/21
Average roughness obtention	05/29/21	05/31/21
Assessment and interpretation of res	05/31/21	06/04/21
4. PROJECT FINALIZATION	06/04/21	06/21/21
4.1 Final delivery of the project	06/14/21	06/14/21
4.2 Presentation preparation	06/15/21	06/21/21
4.3 Project presentation	06/21/21	06/21/21

***Fig 44**. Gantt diagram corresponding to the different tasks of the project.*

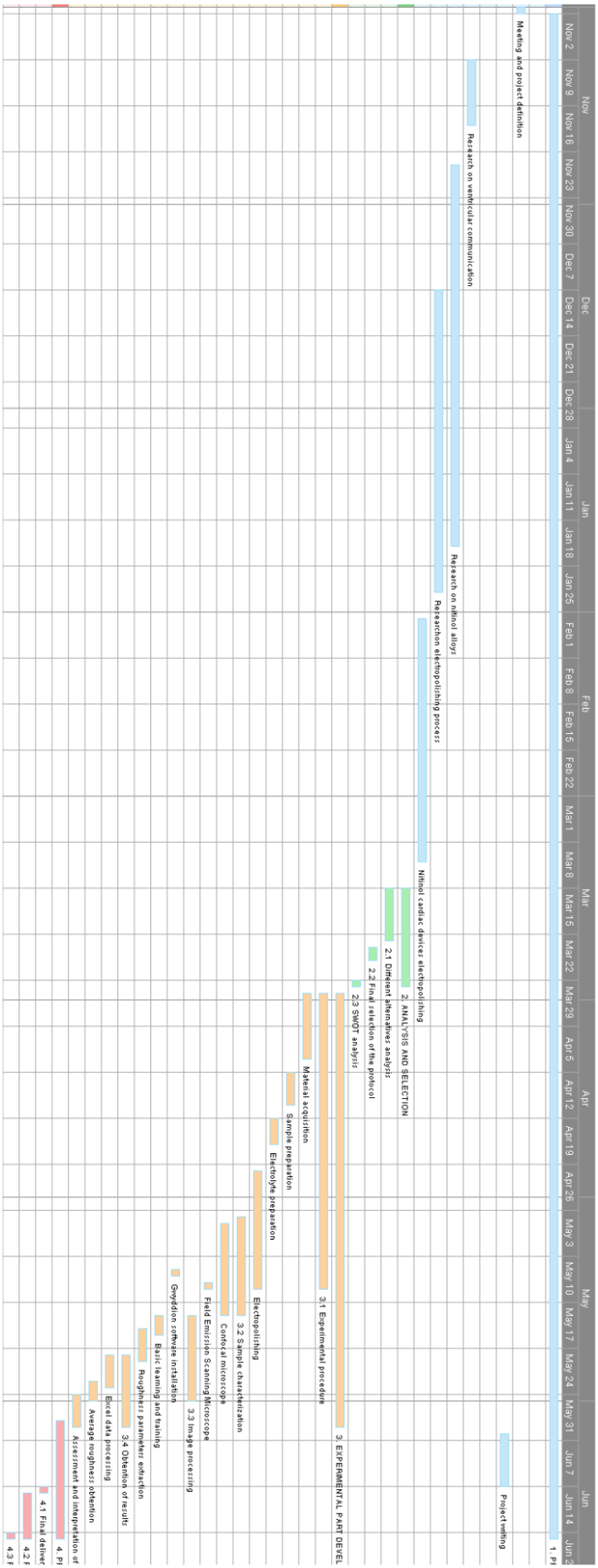

***Fig 45**. Distribution along time of the project tasks..*

7. TECHNICAL FEASBILITY

7.1. STRENGTHS, WEAKNESSES, OPPORTUNITIES AND THREATS (SWOT)

In this section of technical feasibility, the SWOT graph is analysed, a very useful tool which allows to visualize quickly, visually, and intuitively which are those strong and weak aspects that affect the development of the project internally. In addition, it also considers which are the opportunities and threats.

SOT analysis of the project is described below, with the aim of maximizing strengths, minimizing weaknesses and risks while making the most of opportunities to ensure success.

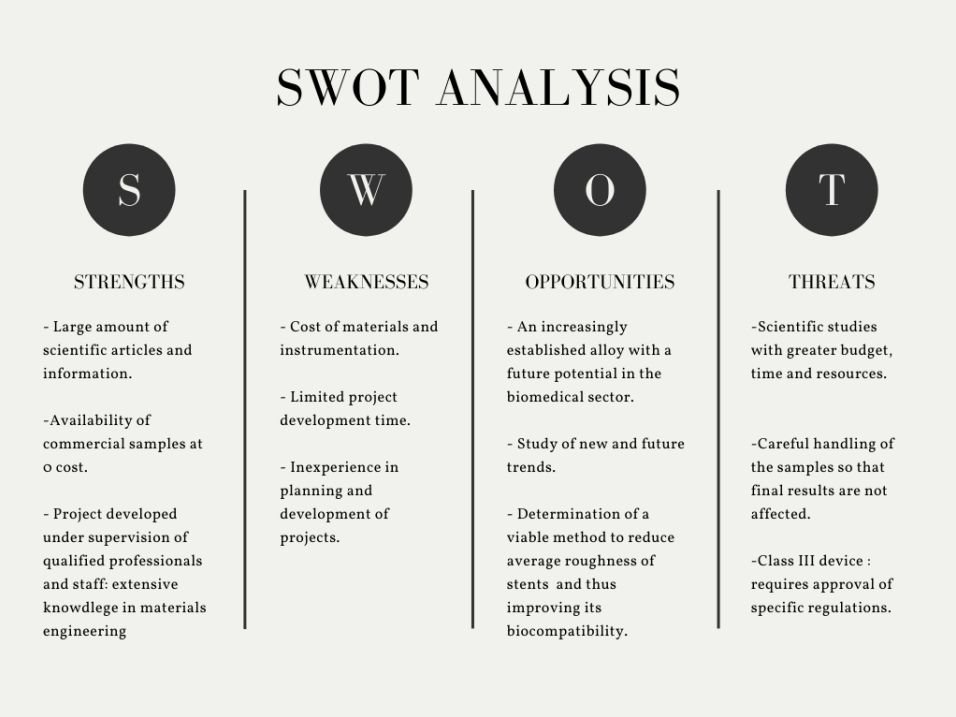

***Fig 46**. SWOT diagram of the project describing its strengths, weaknesses, opportunities, and threats.*

.

- The availability of many sources of information has made it possible to study in detail the nitinol alloy, its properties, and its applications in the biomedical sector, as well as the best techniques to improve the biocompatibility of this material. In addition, working with commercial samples during the experimental procedure has allowed to experience in first person all the concepts learned during the bibliographic and theoretical part. Another important factor to highlight has been the supervision of qualified professionals with extensive knowledge in materials science and engineering, with emphasis on biomedical applications.
- However, in terms of weaknesses, it is worth noting the cost of the materials and all the instruments and devices necessary to carry out the experimental part. Moreover, the limited time of the project must be added, since it has avoided to carry out other types of studies to improve biocompatibility of the samples.

- In terms of opportunities, this project deals with an alloy that is well established in the biomedical field, especially for the treatment of cardiovascular pathologies. As a result, it is a material with a very future potential ahead. Moreover, the project has allowed to discovery and study which are the current trends of this alloy and its future trends. In addition, during the experimental part it has been possible to demonstrate a viable method to reduce average roughness (Ra) of nitinol stents.

- However, it is worth to mention that in many scientific studies with a larger budget and time have been able to achieve a better characterization of this alloy, also having greater availability of resources. In addition, the project also deals with the threat of the approval of specific regulations to ensure its safety. Finally, a careful handling of the samples was required so that results were not affected.

8. ECONOMIC PRE-FEASIBILITY: STUDY OF COSTS AND BUDGETS

This section indicates in detail the economic valuation of this project. The economic items that have been considered are as follows:

8.1 CONSUMABLE MATERIAL

A significant part of the costs of this project is due to the material used. *Table.14.* shows the approximate costs of each of the tasks to be performed during the experimental procedure.

As the **nitinol samples** were provided by an external company that wished to electropolish their cardiac devices, no cost is associated to the material acquisition. Moreover, the **sample preparation** includes the clean-up protocol, which as explained previously, requires specific laboratory instruments as well as reagents such as dodecylbenzenesulfonate. In addition, ethylene glycol for the electrolyte preparation is also included.

Finally, the **electropolishing process** also requires specific devices which also have an associated cost.

EXPERIMENTAL PROCEDURE	QUANTITY	UNIT COST	TOTAL AMOUNT
Nitinol alloy sample	5	0	0
Sample preparation	1	100 €	100
Electropolishing	-	130€	130
		TOTAL:	**230€**

***Table. 14**. Estimated costs associated with the consumable material.*

8.2 HUMAN RESOURCES COSTS

The cost of human resources refers to the cost of the hours spent by the engineer in charge of carrying out this project. In addition, this also includes the hours dedicated by the laboratory supervisor. The role of the supervisor was to coordinate, direct and guide the work to be performed by the engineer in the laboratory.

An associated cost of 20€/hours has been assigned to the engineer and a 45€/hour cost to the laboratory supervisor. Among the total hours required to carry out the project, 150 hours were dedicated by the engineer to perform the experimental procedure in the laboratory.

HUMAN RESOURCES	UNIT	UNIT COST	Nº HOURS	TOTAL AMOUNT (€)
Engineer	Hour (h)	45 €/hour	15	675 €
Laboratory supervisor	Hour (h)	20 €/hour	150	3000 €
			TOTAL:	**3675 €**

***Table. 15**. Estimated human labour costs for the project development.*

8.3 CHARACTERIZATION EQUIPMENT COSTS

This section includes the costs of using image characterization equipment, including the Confocal Microscopy and the Field Emission Scanning Electron Microscopy. *Table.16.* shows the costs of these equipment that have been necessary for the study analysis and sample imaging.

It is important to mention that the FESEM was in the Scientific and Technologic Centre, which is affiliated to the university of Barcelona. Therefore, due to the existence of agreements and agreements between the two institutions, the total cost turned out to be cheaper. In order to assign the unit cost of these equipment, a document with different rates was consulted [56].

CHARACTERIZATION EQUIPMENT	UNIT	UNIT COST	Nº HOURS	TOTAL AMOUNT(€)
Confocal Microscopy	Hour (h)	10,33 €/hour	12	123,96€
FESEM	Hour (h)	73,6 €/hour	3	220,8€
			TOTAL:	**334,76€**

***Table. 16**. Estimated costs of the characterization equipment.*

Now that the breakdown of the different costs has been made, it is possible to obtain an approximation of the total project cost.

TOTAL PROJECT INVESTMENT	
Consumable material	**230€**
Characterization equipment	**334,76€**
Human labour	**3675 €**
TOTAL:	**4239,76 €**

***Table. 17**. Summary of the total project investment.*

As shown in *Table. 2.*, the total estimated cost of the project is **4239,76 €**.

It is important to clarify that, in different circumstances, the total cost of the same would have been much higher since the costs of each of the economic items considered would rise.

For instance, the samples have been obtained at cost 0 since they were provided by an external company whose intention was to perform an electropolishing process. In other circumstances, the samples would have had to be purchased, considerably increasing the cost.

Moreover, the existence of agreements between the University of Barcelona and other entities has made it possible to reduce costs in terms of the use of equipment for the characterization of the samples. Without the existence of these agreements, the costs would have been much higher.

9. REGULATIONS AND LEGAL ASPECTS

9.1 MAIN REGULATIONS

This section includes the main regulations and legal aspects associated with the development of this project.

As dealing with medical devices, these are obliged to pass through the approval of the different regulations, to ensure a proper quality and safety to human health. There are four risk classes associated to these devices: risk III, IIb, IIa and I, from highest to lowest risk. This classification system is a risk-based system and the fundamental criteria it considers are the degree of invasiveness of the product, the part of the organism which is in contact and the duration of this contact [57].

More specifically, cardiac devices such as vascular stents or heart valves are classified as class III devices, due to the level of risk associated and its invasiveness [58]. The organism that regulates and controls medical devices in the United States is the Food and Drug Administration (FDA). This organism has determined that general and special controls alone are insufficient to assure the safety and effectiveness of Class III devices. Therefore, they require a premarket approval (PMA) application under section 515 of the FD&C Act in order to obtain marketing approval [59].

On the other hand, it is important to consider that the legislation of these devices is different depending on the country.

In Spain, the regulation of medical devices is given by the following royal decrees:

- Royal decree 1591/2009, of 16 October, which regulates the sanitary products and medical devices [60].

- Royal decree 1616/2009, of 26 October, which regulates active implantable medical devices [61].

Regarding the placing on the market of medical devices within the framework of the European Union, the manufacturer of a medical device must contact the notified bodies. These are organisations designated by the countries of the European Union themselves. Manufacturers must come presenting documentation on the design, manufacturing and sterilization processes, performance tests, technical standards that the product complies with, among other aspects. [62]

Once the verification of the documentation is favourable, the product will obtain the CE mark, indicating that it complies with all the regulatory requirements.

In Spain, the Notified Body responsible of performing this procedure is the General Directorate of Pharmacy and Medical Devices [62].

9.2 ISO STANDARDS

Cardiovascular devices such as stents or heart valves are classified as class 3 devices due to its invasiveness and risks associated. Consequently, it is important to mention the ISO quality and reliability standards associated with these medical devices.

- **ISO 13485**: Internationally recognized standard for quality management systems in the medical device industry. Having this standard can help expand the potential market and bring benefits to regulatory approval in important markets such as the European Union and Canada [63].

- **ISO 13485:2016**: This new version of the previous one consists of a manual that aims to guide organizations in the development, implementation and maintenance of their quality management system in accordance with ISO 13485 [63].

- **ISO 14971**: Application of risk management to medical devices. By means of this procedure, the manufacturer can identify the risks associated with his medical devices and their accessories [64].

10. CONCLUSIONS AND FUTURE LINES

10.1 CONCLUSIONS

This final degree project has led to the following conclusions:

- **Nitinol is a SMA with unique properties** which make this material of special interest in many biomedical applications.

- **Cardiovascular nitinol-based devices** such as vascular stents or heart valves can be used to treat certain cardiovascular pathologies.

- **Surface quality** of nitinol stents plays a decisive role in terms of their biocompatibility.

- **Electropolishing** is a surface treatment which demonstrates high efficacy in reducing the average roughness (Ra) of nitinol stents.

As for the experimental procedure carried out, the following conclusions are considered:

- The process of electropolishing nitinol cardiac samples has been optimized using **ethylene glycol – sodium chloride as electrolyte**. A concentration of NaCl of 1mol/L and a concentration of distilled water of 1 vol.% were used.

- The electropolishing conditions found as optimal have been the following: **a voltage of 22.5V at room temperature (22ºC) for a total time of 5 minutes.**

- The minimum Ra value obtained was **47.821283 nm ± 19.4495**, thus achieving a reduction in average roughness (Ra) of **97.4%** compared to the original samples.

10.2 FUTURE LINES

Due to the time limitation of the project, it has not been possible to carry out some procedures which were initially planned. These procedures would have allowed to perform a more complete and in-depth study of nitinol alloy and its biocompatibility. Therefore, as future lines related to this project, it can be highlighted:

- The creation and growth of a TiO_2 layer of by means of chemical or physical procedures. The main purpose of this layer is to reduce the emission and diffusion of Nickel ions through the surface of the implant. As a result, due to the biocompatibility problems associated to nickel, possible adverse reactions in patients would be avoided.

- Other alternative process to achieve the elimination of Nickel on the surface of the material. As previously explained, the main goal is to prevent nickel to be released into the outer environment and surrounding tissues. Two examples of these processes would be chemical etching and Physical vapor deposition (PVD).

11. BIBLIOGRAPHY

[1] K. Sangeetha, A. V. J. Kumari, J. Venkatesan, A. Sukumaran, S. Aisverya, and P. N. Sudha, *13. Degradable metallic biomaterials for cardiovascular applications*, no. April 2019. Elsevier Ltd, 2018.

[2] J. B. Osorno, "Biomateriales de uso cardiovascular."

[3] C. Wen, X. Yu, W. Zeng, S. Zhao, L. Wang, and G. Wan, *Mechanical behaviors and biomedical applications of shape memory materials : A review*, vol. 5, no. June. 2018.

[4] M. Behl and A. Lendlein, "Shape-memory polymers are an emerging class of active polymers that," *Mater. Today*, vol. 10, no. 4, pp. 20–28, 2007, doi: 10.1016/S1369-7021(07)70047-0.

[5] H. Holman *et al.*, "Smart Materials in Cardiovascular Implants: Shape Memory Alloys and Shape Memory Polymers," pp. 0–2, doi: 10.1111/aor.13851.

[6] D. S. Levi, N. Kusnezov, and G. P. Carman, "Smart materials applications for pediatric cardiovascular devices," *Pediatr. Res.*, vol. 63, no. 5, pp. 552–558, 2008, doi: 10.1203/PDR.0b013e31816a9d18.

[7] S. Shabalovskaya, J. Anderegg, and J. Van Humbeeck, "Critical overview of Nitinol

surfaces and their modifications for medical applications," vol. 4, pp. 447–467, 2008, doi: 10.1016/j.actbio.2008.01.013.

[8] A. Whitepaper, "The Advantages of Electropolishing for Deburring Metal Parts Highlights of this Whitepaper :," 2001.

[9] H. N. Filho, M. Tereza, F. Soares, and H. D. Nagem, "Surface Roughness of Composite Resins After Finishing and Polishing," vol. 14, pp. 37–41, 2003.

[10] J. R. Beramendi Calero *et al.*, "Comunicacion inteventricular en la edad neonatal," *An. Esp. Pediatr.*, vol. 49, no. 3, pp. 284–288, 1998.

[11] M. S. Minette and D. J. Sahn, "Ventricular septal defects," *Circulation*, vol. 114, no. 20, pp. 2190–2197, 2006, doi: 10.1161/CIRCULATIONAHA.106.618124.

[12] C. Mavroudis and J. A. Dearani, *Atlas of Adult Congenital Heart Surgery*. 2020.

[13] J. Zhang, J. M. Ko, J. M. Guileyardo, and W. C. Roberts, "A Review of Spontaneous Closure of Ventricular Septal Defect," *Baylor Univ. Med. Cent. Proc.*, vol. 28, no. 4, pp. 516–520, 2015, doi: 10.1080/08998280.2015.11929329.

[14] M. E. Menting *et al.*, "The unnatural history of the ventricular septal defect: Outcome up to 40 years after surgical closure," *J. Am. Coll. Cardiol.*, vol. 65, no. 18, pp. 1941–1951, 2015, doi: 10.1016/j.jacc.2015.02.055.

[15] J. Yang *et al.*, "Transcatheter versus surgical closure of perimembranous ventricular septal defects in children: A randomized controlled trial," *J. Am. Coll. Cardiol.*, vol. 63, no. 12, pp. 1159–1168, 2014, doi: 10.1016/j.jacc.2014.01.008.

[16] T. R. Study, "Determinants of Peripheral Arterial Disease in the Elderly," vol. 160, 2015.

[17] S. Subherwal *et al.*, "Peripheral artery disease is a coronary heart disease risk equivalent among both men and women : results from a nationwide study," 2015, doi: 10.1177/2047487313519344.

[18] F. J. Serrano and A. Martín, "Enfermedad arterial periférica : aspectos fisiopatológicos , clínicos y terapéuticos," *Rev. española Cardiol.*, vol. 60, no. 9, pp. 969–982, 2007, doi: 10.1157/13109651.

[19] N. B. Morgan, "Medical shape memory alloy applications — the market and its products," vol. 378, pp. 16–23, 2004, doi: 10.1016/j.msea.2003.10.326.

[20] M. Azaouzi, A. Makradi, and S. Belouettar, "Deployment of a self-expanding stent inside an artery: A finite element analysis," *Mater. Des.*, vol. 41, pp. 410–420, 2012, doi: 10.1016/j.matdes.2012.05.019.

[21] M. Drobac, N. Kostic, and D. Vasiljevic, "Vascular stents : The most important types and characteristics Vaskularni stentovi – najzna č ajnije vrste i osobine," no. December 2015, 2014, doi: 10.5937/arhfarm1405421D.

[22] A. Pelton, "Self-expanding nitinol stents : material and design considerations," no. December 2009, 2020, doi: 10.1007/s00330-003-2022-5.

[23] A. Szold, "Nitinol: Shape-memory and super-elastic materials in surgery," *Surg. Endosc. Other Interv. Tech.*, vol. 20, no. 9, pp. 1493–1496, 2006, doi: 10.1007/s00464-005-0867-1.

[24] M. B. Popovic, K. A. Lamkin-kennard, P. Beckerle, and M. P. Bowers, *3.1 Introduction*. 2019.

[25] J. Mohd, M. Leary, A. Subic, and M. A. Gibson, “A review of shape memory alloy research , applications and opportunities,” *Mater. Des.*, vol. 56, pp. 1078–1113, 2014, doi: 10.1016/j.matdes.2013.11.084.

[26] D. E. Hodgson, S. M. Applications, M. H. Wu, and M. Corporation, “Shape Memory Alloys,” vol. 2.

[27] G. B. Kauffman and I. Mayo, “No Title,” vol. 2, no. 2, pp. 1–21, 1996.

[28] B. Weber *et al.*, “Iron-based shape memory alloys for civil engineering structures An overview Iron-based shape memory alloys for civil engineering structures : An overview,” *Constr. Build. Mater.*, vol. 63, no. August, pp. 281–293, 2014, doi: 10.1016/j.conbuildmat.2014.04.032.

[29] M. Okrasa, “Preliminary study on the thermomechanical treatment of shape memory alloys for applications in clothing protecting against heat,” vol. 9, no. 6, pp. 1–9, 2017, doi: 10.1177/1687814017703898.

[30] U. N. B. Con, I. Algo, G. López, M. I. Felipe, and C. Rodríguez, “Facultad de estudios superiores cuautitlán,” 2011.

[31] T. Bormann, S. Friess, M. de Wild, R. Schumacher, G. Schulz, and B. Müller, “Determination of strain fields in porous shape memory alloys using micro-computed tomography,” *Dev. X-Ray Tomogr. VII*, vol. 7804, no. May 2014, p. 78041M, 2010, doi: 10.1117/12.861386.

[32] T. G. Gangadhar, K. Manickavelan, and B. Singh, “Analysis of Fatigue Behaviour of Superelastic Nitinol Wires,” vol. 4, no. 9, pp. 7–18, 2015.

[33] S. A. Shabalovskaya, “Surface , corrosion and biocompatibility aspects of Nitinol as an implant material,” vol. 12, pp. 69–109, 2002.

[34] D. Batalu and X. Liu, “A review on TiNi shape memory alloys (SMA) used for medical applications . Recycling aspects A review on TiNi shape memory alloys (SMA) used for medical applications . Recycling aspects,” no. November 2014.

[35] D. Stoeckel, A. Pelton, and T. Duerig, “Self-Expanding Nitinol Stents - Material and Design Considerations,” 2003.

[36] “Nitinol Stents in the Femoropopliteal Artery_ A Mechanical Perspective on Material, Design, and Performance _ Enhanced Reader.pdf.” .

[37] A. R. Pelton, J. Dicellol, and S. Miyazaki, “Optimisation of processing and properties of medical grade Nitinol wire,” vol. 9, no. 1, pp. 107–118, 2000.

[38] H. R. Wang, F. Liu, Y. P. Zhang, D. Z. Yu, and F. P. Wang, “Preparation and properties of titanium oxide film on NiTi alloy by micro-arc oxidation,” *Appl. Surf. Sci.*, vol. 257, no. 13, pp. 5576–5580, 2011, doi: 10.1016/j.apsusc.2011.01.047.

[39] L. Geyao, D. Yang, C. Wanglin, and W. Chengyong, “Development and application of physical vapor deposited coatings for medical devices: A review,” *Procedia CIRP*, vol. 89, pp. 250–262, 2020, doi: 10.1016/j.procir.2020.05.149.

[40] J. Kim, J. K. Park, H. K. Kim, A. R. Unnithan, C. S. Kim, and C. H. Park, “Optimization of electropolishing on NiTi alloy stents and its influence on corrosion behavior,” *J. Nanosci. Nanotechnol.*, vol. 17, no. 4, pp. 2333–2339, 2017, doi: 10.1166/jnn.2017.13324.

[41] W. D. Miao, X. J. Mi, X. L. Wang, and H. C. Li, “Electropolishing parameters of NiTi alloy,”

Trans. Nonferrous Met. Soc. China (English Ed., vol. 16, no. SUPPL., pp. 0–2, 2006, doi: 10.1016/S1003-6326(06)60160-X.

[42] W. Han and F. Fang, "Fundamental aspects and recent developments in electropolishing," *Int. J. Mach. Tools Manuf.*, vol. 139, no. December 2018, pp. 1–23, 2019, doi: 10.1016/j.ijmachtools.2019.01.001.

[43] X. Sun, X. Wei, Z. Li, D. Lou, Y. Wang, and H. Liu, "Electrochemistry," pp. 15–19, 2020, doi: 10.5796/electrochemistry.20-00047.

[44] I. De Scheerder *et al.*, "Metallic surface treatment using electrochemical polishing decreases thrombogenicity and neointimal hyperplasia of coronary stents," *J. Interv. Cardiol.*, vol. 13, no. 3, pp. 179–185, 2000, doi: 10.1111/j.1540-8183.2000.tb00286.x.

[45] E. S. Lee and T. H. Shin, "An evaluation of the machinability of nitinol shape memory alloy by electrochemical polishing," *J. Mech. Sci. Technol.*, vol. 25, no. 4, pp. 963–969, 2011, doi: 10.1007/s12206-011-0209-2.

[46] W. Simka, M. Kaczmarek, A. Baron-Wiecheć, G. Nawrat, J. Marciniak, and J. Zak, "Electropolishing and passivation of NiTi shape memory alloy," *Electrochim. Acta*, vol. 55, no. 7, pp. 2437–2441, 2010, doi: 10.1016/j.electacta.2009.11.097.

[47] E. Kassab *et al.*, "On the electropolishing of NiTi braided stents - Challenges and solutions," *Materwiss. Werksttech.*, vol. 45, no. 10, pp. 920–929, 2014, doi: 10.1002/mawe.201400220.

[48] D. M. Whelan, W. J. Van Der Giessen, S. C. Krabbendam, E. A. Van Vliet, and P. D. Verdouw, "Biocompatibility of phosphorylcholine coated stents in normal porcine coronary arteries," pp. 338–345, 2000.

[49] B. Thierry, M. Winnik, Y. Merhi, and J. Silver, "Bioactive Coatings of Endovascular Stents Based on Polyelectrolyte Multilayers," pp. 1564–1571, 2003.

[50] A. L. Lewis, L. A. Tolhurst, and P. W. Stratford, "Analysis of a phosphorylcholine-based polymer coating on a coronary stent pre- and post-implantation," vol. 23, pp. 1697–1706, 2002.

[51] P. Batra and J. M. Islamia, "Total Recall : An Update On Orthodontic Wires," no. September, 2014.

[52] W. A. Gray *et al.*, "CLINICAL STUDY S . M . A . R . T . Self-Expanding Nitinol Stent for the Treatment of Atherosclerotic Lesions in the Superficial Femoral Artery (STROLL): 1-Year Outcomes," *J. Vasc. Interv. Radiol.*, pp. 1–8, 2014, doi: 10.1016/j.jvir.2014.09.018.

[53] W. D. Fremont, "We are Nitinol . ™."

[54] C. Bonsignore, "Present and Future Approaches to Lifetime Prediction of Superelastic Nitinol Present and future approaches to lifetime prediction of superelastic nitinol," *Theor. Appl. Fract. Mech.*, vol. 92, no. April, pp. 298–305, 2017, doi: 10.1016/j.tafmec.2017.04.001.

[55] K. Fushimi, M. Stratmann, and A. W. Hassel, "Electropolishing of NiTi shape memory alloys in methanolic H2SO4," *Electrochim. Acta*, vol. 52, no. 3, pp. 1290–1295, 2006, doi: 10.1016/j.electacta.2006.07.030.

[56] P. Cleaner and M. Aligner, "Plataforma de nanotecnología - tarifes 2014," pp. 9–10, 2014.

[57] L. Peter, L. Hajek, P. Maresova, and M. Augustynek, “Medical Devices : Regulation , Risk Classification , and Open Innovation,” no. Mdi, 2020.

[58] D. E. P. Sanitarios, “www.aemps.es .,” 2010.

[59] D. B. Kramer, S. Xu, M. Sc, and A. S. Kesselheim, “H e a l t h L a w , E t h i c s , a n d H u m a n R i g h t s Regulation of Medical Devices in the United States and European Union,” 2012.

[60] I. D. Generales, “Boletín oficial del estado,” pp. 92708–92778, 2009.

[61] I. D. Generales, “Boletín oficial del estado,” pp. 92779–92823, 2009.

[62] “Documento de instrucciones de la Agencia Española de Medicamentos y Productos Sanitarios para la realización de ensayos clínicos en España documento debe dirigirse a la dirección de correo electrónico aecaem@aemps.es citando,” pp. 1–43, 2019.

[63] D. E. Implementaci, D. E. S. D. E. Gesti, D. E. C. En, and P. Sanitarios, “Iso 13485:2016 50,000,” 2016.

[64] U. Iso, E. Del, and D. U. Iso, “Norma Española Dispositivos médicos / productos sanitarios (MD) Aplicación de la gestión del riesgo a los MD,” 2020.

12. ANNEXES

12.1 PROTOCOL TO FOLLOW

1- Opening of the software and the desired image. From the main menu, *File* and *Open* had to be selected in order to load the corresponding images to be processed.

2- Once the desired image has been opened, the Data Browser window displays two images to be processed, Topography and Gray. Among these two, the topography image had to be chosen.

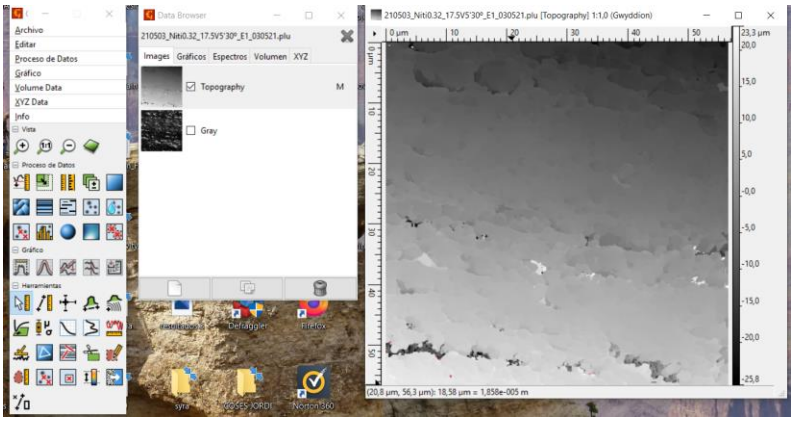

***Fig 47**. Opening of the topography image to be processed.*

3- The next step consisted in changing the pixel scale of the image which comes by default to the physical scale., by selecting this option in the upper left corner of the image.

4- Then, the tonality of colours of the image was modified to be able to appreciate in a more detailed way the differences in height of our image. To do this, the right mouse button had to be clicked above the vertical axis Z of the image. Consequently, the Gwyddion.net tonality of colours was selected.

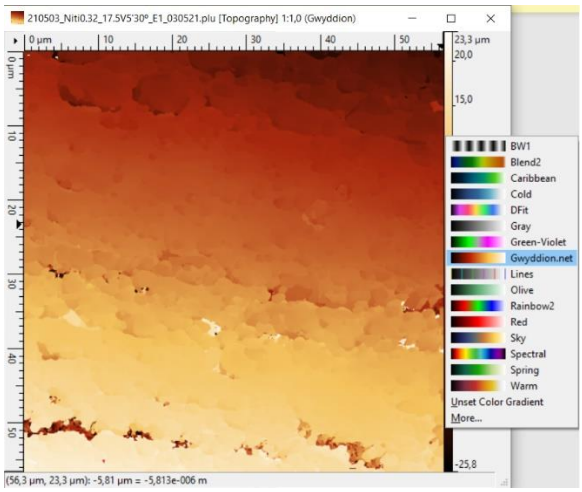

Fig 48. *Changing the tonality of colours to Gwyddion.net.*

5- The next step consisted in selecting the *Level Data by Mean Plane Substraction* option in the tool's menu. With this option, the software considers the image to be flat.

6- Afterwards, the *Read Value Under Mouse Cursor* option was selected. With this option, a value of 0 in the scale is given to any desired point of the image, and , as a result, the Z axis is changed according to the selected spot.

7- At this point, the image is already prepared and ready to assess the roughness parameters. The *Calculate Roughness Parameters* option had to be selected from the tool's menu.

7.1

Once this option is selected, the roughness of the sample is calculated. To perform this process, a horizontal line is drawn along the entire sample.

7.2

In the window next to the image, different roughness parameters will appear. A *Cut-off* of 0.1 is set and *Apply* is selected in order to visualize the corresponding roughness graph.

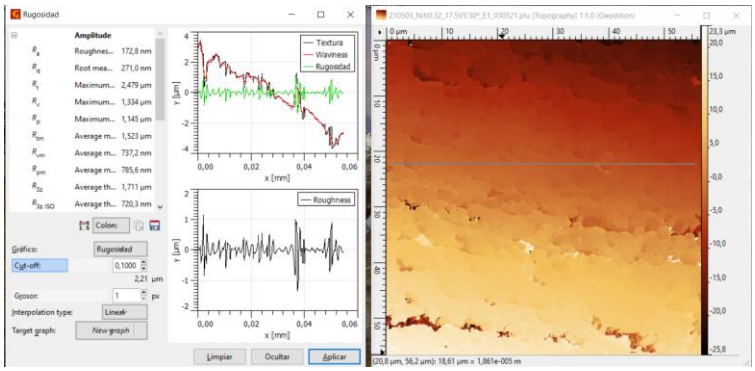

***Fig 49**. Horizontal line drawn along the sample to obtain roughness parameters.*

7.3 With the right mouse button, *Align* and *Level* options are selected. As the name suggests, these options allow to align and level the image. The image is then saved and exported by selecting *Export Bitmap* option

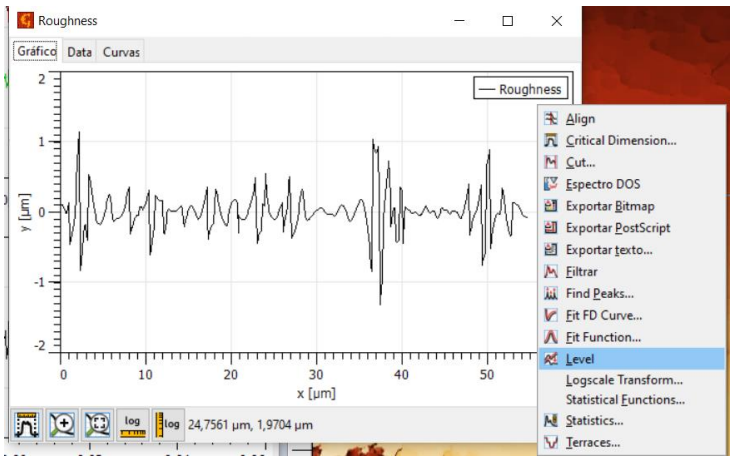

***Fig 50**. Visualization of the roughness graph after being aligned and levelled.*

7.4 Finally, the roughness parameters which had appeared in the previous window are also exported so that they can be processed later by using the Excel Software.